PATENT SPECIFICATION

(11) **1 424 689**

(19)

(54) IMPROVEMENTS IN OR RELATING TO HEAT EXCHANGERS

(71) We, UNION CARBIDE CORPORATION, a corporation organised and existing under the laws of the State of New York, United States of America, of 270 Park Avenue, New York, State of New York 10017, United States of America, (assignee of LESLIE CHARLES KUN), do hereby declare the invention, for which we pray that a patent may be granted to us, and the method by which it is to be performed, to be particularly described in and by the following statement:—

This invention relates to heat exchangers and has particular application to a heat exchanger having channels as primary surfaces and fins attached to the channels as the secondary surfaces.

In cross flow heat exchangers for waste heat rejection from internal combustion engines, power plants and the like, a first coolant fluid (e.g. water) is cooled inside the heat exchanger passages by rejecting heat to a second fluid (e.g. air) flowing in spaces outside and between the passages. These exchangers are constructed with both primary and secondary heat exchange surface. Primary surfaces are those which bound the passage walls separating the two fluids in heat exchange. The metallic flow path between the fluids is merely the thickness of the passage wall so that heat flow is substantially normal to the wall. In contrast, secondary surfaces are those which bound metal extensions from primary surfaces and such extensions are substantially surrounded by only one of the fluids. Accordingly, the heat flow path through the secondary surface is substantially parallel to the surface.

In the above-mentioned cross flow heat exchanger, the first fluid (coolant) heat transfer film coefficients inside the primary passages are many times greater than the second fluid (air) heat transfer film coefficients on the primary and secondary surfaces so that the latter represents the controlling or limiting resistance to heat transfer. For example, in a typical automobile radiator with the vehicle operating at cruising speed, the first fluid co-

efficient may be 1300 BTU/hr.×°F. whereas the air-side coefficient may be only 30—50 BTU/hr.×ft²×°F. Because of this wide disparity in coefficients a large area of secondary surface has been employed on the air side and typical area ratios, air side/coolant side are between 8 to 1 and 10 to 1. In prior art radiators as illustrated in Fig. 20, the secondary surface has been provided in the form of sheet metal fins which are stacked or folded in closely spaced relationship with flattened tubes (primary surfaces) piercing through apertures in the fins or inter-fitted between strips of folded fin metal. In general, the prior art has evenly distributed such large areas of secondary surface metal over the surface of the primary tube wall. Otherwise if the primary wall is thin, lateral temperature gradients will develop in the tube wall near the points of attachment of secondary material and will in effect further lengthen the heat flow path between the two fluids.

The prior art has usually employed copper or copper alloy in the fabrication of radiator-type cross flow heat exchangers, and brazing or soldering have been used to metallically bond the secondary surface to the primary wall thereby minimizing thermal resistance of the joint to heat transfer. As an indication of the state-of-art, a brazed copper automobile radiator having a secondary surface/primary surface area ratio of between 8 and 10 to 1 may employ about 2.7 lbs. of metal to transfer 1000 BTU heat per minute at highway driving conditions. For this quantum of heat transfer capacity the metal cost will be used as a comparison base and assigned a value of 1.0.

Because of the trend towards higher pressure operation in automobile radiators and the inherent stress limitations of thin-wall copper construction, there is considerable impetus for substitution of aluminum, particularly in view of its low cost, high thermal conductivity, and availability in tubes and thin sheets. However, aluminum surfaces oxidize readily and the metal is difficult to bond by brazing or soldering either to itself or to other materials. It has

proved extremely difficult to produce the extensive and relatively inaccessible bonds for attachment of secondary-to-primary heat transfer material for aluminum radiators as contrasted to copper. Notwithstanding these difficulties, aluminum automobile radiators of the conventional secondary surface type of Fig. 20 have been produced and evaluated. Such an exchanger having an area ratio of between 8 and 10 to 1 would typically employ about 1.97 lbs. of metal to transfer 1000 BTU heat per minute at highway driving conditions. The lower weight compared to the soldered copper radiator reflects lower density of aluminum relative to copper. For this quantum of heat transfer capacity, the metal cost would be about 0.39 of the copper radiator metal cost. Thus, the combination of lower density and lower cost of heat per minute affords a much lower cost radiator when produced of aluminum rather than copper.

It is emphasized however that the prior art has not substantially solved the problem of making the necessary bonds in an aluminum radiator having the same configuration as the presently used copper radiators. The aforementioned problems are partially circumvented by the use of a substantially all primary surface aluminum heat exchanger fabricated from thin sheet metal and employing a multiplicity of wall projection portions formed from each side wall, being distributed across the side wall surface and extending outwardly therefrom. These projections have load-bearing end segments used for mating with and abutting against load bearing end segments of wall projections extending outwardly from adjacent primary surface channel side walls. An outer structural frame is provided and the outermost end segments of the primary surface wall projection portions bear against the outer structural frame. In this manner the load of the sandwiched channel assembly is transferred to the outer frame.

One form of such wall projection portions is described and claimed in our copending British Patent application No. 47237/72 (Serial No. 1403063) filed October 13th 1972.

These wall projection portions are in the form of outwardly extending truncated cones having a dimensional size and a dimensional relationship defined by a H/D ratio of 0.05—0.2, a D/d ratio of 3—10, and a D dimension of 0.2—2.5 inches, a R/D ratio greater than about 0.075, and a cone angle of less than 35°. In the aforedefined relationship H is the distance from each load-bearing end segment to the plane of the side wall surface in a direction perpendicular to said plane, D equals the spacing between the centers of the closest adjacent wall-supporting projections on the surface of the wall, d equals the equivalent diameter defined by the ratio of $4a/p$ in which a equals the area of the load bearing end segment of the wall projection portion and p

equals the perimeter of such load bearing end segment, the cone angle equals the acute angle measured between the horizontal undeformed surface of the wall adjacent the projection and the substantially straight segment along the sloped side of the projection, and R equals the radium of curvature of the surface segments on both sides of the bonding line of intersection formed by the projection and the undeformed surface of the wall adjacent the projection.

Another form of such wall projection portions is described and claimed in our copending British Patent application No. 47238/72 (Serial No. 1412442) filed October 13th 1972.

These wall projection portions are in the form of outwardly extending isostress contours having a dimensional size and a dimensional relationship defined by a H/D ratio of 0.05—0.2, a D/d ratio of 3—10 and a D dimension of 0.2—2.5 inches. In the aforedefined relationships H equals the maximum height measured perpendicularly from a surface which contains the extremities of the projections enclosing an isostress contour to the innermost crest of the isostress contour, and the D and d dimensions are the same as previously defined for the truncated conical projection portions.

Despite the fact that primary metal is contacted by the high-resistance air film on the outer side only, the overall heat transfer capability of all primary surface aluminum heat exchangers employing the above described wall projection portions is equivalent to that of the conventional copper radiator with a large area of secondary surfaces. Without the need for secondary surfaces such as fins, the use of aluminum as a construction material for cross flow radiator heat exchangers is entirely feasible. The total length of the metal-to-metal joints is greatly reduced, all bonds and joints are substantially isothermal, and therefore it can be bonded by adhesives. Much of the remaining joint length of such all-primary surface aluminum heat exchanger, i.e. the longitudinal channel seams, may be prefabricated before assembly and is readily accessible. By way of example, an aluminum automobile radiator of the type described in our British Patent application No. 47238/72 (Serial No. 1412442) with isostress contoured wall projection portions and having an area ratio (air side/water side) of 1.0 would employ 2.94 lbs. metal to transfer 100 BTU per minute at highway driving conditions. For this quantum of heat transfer capacity the metal cost would be about 0.59 of the copper radiator metal cost. It is evident from this comparison that this all-primary surface aluminum heat exchanger represents an attractive alternative to the brazed secondary surface aluminum exchanger. Not only does it successfully eliminate the brazing problem heretofore associated with the use of aluminum but it also approaches the metal economy achievable with the brazed aluminum radiator (metal cost of 0.59 as com-

pared with 0.39 for the latter).

Unfortunately, further improvement in the metal economy of the all-primary surface aluminum heat exchanger is severely limited by strength, manufacturing, corrosion and air side plugging problems. The wall thickness may be reduced by increasing the number of wall projection portions having load-bearing end segments, but this in turn increases the air flow resistance and reduces the rate of air flow. This undesirable effect is amplified if the height H of the wall projection portion is reduced in proportion to the projection spacing D since the spacing between adjacent primary surface channels is thereby reduced. Moreover reductions in metal wall thickness are ultimately limited by minimum thickness necessary to accommodate unavoidable aluminum erosion and corrosion, and by minimum sheet thickness which can be handled, fabricated and employed in radiator service without mechanical damage. Reduction in the air side passage width of automobile radiators is also limited because of the tendency of airborne debris to plug the passages.

An object of this invention is to provide an aluminum cross flow heat exchanger of the primary surface-wall projection load supporting type.

Another object of this invention is to provide such a heat exchanger having at least equivalent metal economy as compared to a brazed aluminum exchanger having conventional secondary fin surface.

Still another object is to provide an aluminum radiator suitable for a motor vehicle.

The cross flow heat exchanger of this invention comprises an outer structural frame; a multiplicity of channels formed of aluminum each having an elongated cross section bound by side walls and edge walls each of between 0.003 and 0.015 inch thickness and an aspect ratio of length to width of an equivalent rectangle equal to at least 4, said channels being longitudinally aligned in parallel spaced relation each with a first fluid entrance opening at one end and a first fluid exit opening at the opposite end, and common inlet manifold means respectively for said first fluid entrance openings and said first fluid exit openings, and a multiplicity of wall projection portions formed from each side wall being distributed across the side wall surface and extending outwardly therefrom with load-bearing end segments shaped for mating with and abutting against load-bearing end segments of said projection portions of an adjacent channel side wall thereby spacing adjacent channels with the outermost end segments bearing against and transferring the channel load to said outer structural frame, said wall projection portions having a dimensional size and a dimensional relationship therebetween defined by a D dimension of between about 0.2 and 1 inch, an H dimension of between about 0.02 and

0.14 inch, and a D/d ratio of between about 3 and 18 wherein H is the distance from each load-bearing end segment to the plane of the side wall surface in a direction perpendicular to said plane, D equals the effective spacing between the centers of adjacent wall projection portions of a side wall as determined by the formula:

$$D = 3\sqrt{\frac{D_1{}^3 + D_2{}^3}{2}}$$

wherein D_1 = shortest distance between two adjacent wall projection portions in any triangular unit of the projection pattern on the side wall, D_0 = perpendicular distance from a straight line extending through said two adjacent wall projection centers to the center of the third wall projection of the same triangular unit, triangular unit = a triangle having a wall projection center only at each of its apexes with each side of the triangle extending between wall projection centers without transversing a shorter line segment interconnecting other projection centers, and d equals the dimension of the ratio $4a/p$ wherein a equals the area of the load-bearing end segment of the wall-supporting projection and p equals the perimeter of said load-bearing end segment and said wall projection portions also having an elevational contour such that the ratio θ/R is between about 4 and 2500 degrees/inch wherein θ is the maximum angle of metal in the projection portion with respect to the base plane of said side wall and measured in a cross section passing through the projection portion center perpendicular to the base plane, and R is the minimum radius of curvative of said metal measured outside the projection portion; said channels and wall projection portions thereby, and outer structural frame being arranged and constructed for flowing a second fluid through said outer structural frame normal to and in the space between said channels in heat exchange with said first fluid; and at least one thin aluminum fin of between 0.003 and 0.015 inch thickness extending at least outwardly from an edge wall of each channel along the entire length thereof, said fins being provided in number and surface area relative to the channel surface area such that the ratio $(O_0 + O_p)/I_x$ of channel outer surface area (O_0) plus fin surface area outside said channels (O_p) to total surface area inside said channels (I_x) is between 1.2 and 4.0, and with each fin having a multiplicity of surface distortions from the fin plane into the gap between adjacent fins of adjacent channels being closely spaced at intervals (S) between 0.01 and 0.2 inch measured normal to the channel longitudinal axis, so as to comprise a total distortion area which is at least 40% of said fin surface area thereby disrupting the second fluid film across the fin width.

1,424,689

This invention requires the addition of thin thermally conductive sheet metal fins as secondary heat transfer surfaces to the primary surface channels. However, fins can only be added along the narrow longitudinal edges of each channel because the close spacing of adjacent channels precludes fin attachment on other areas of the channels, e.g. the side walls. That is, for the large required primary surface area in a useful cross flow radiator-type heat exchanger, the channel side walls must be closely spaced to define narrow first and second fluid passages as for example 40—150 each of first and second fluid passages per foot of heat exchanger cross section. Also in order to provide a substantial cross-sectional flow area for the second fluid between the channels, the channel side walls must be essentially flat. Accordingly, the geometry of the cross flow heat exchanger is such that the narrow longitudinal edge walls of each channel are the only portions of the channel which are not closely confined within the assembled heat exchanger.

Despite the foregoing limitations and the lateral temperature gradient in the primary surface channels which attachment of secondary surface fins unavoidably produces, the instant heat exchanger has been demonstrated to afford at least a 50% improvement in heat transfer performance as compared to the previously described all-primary surface heat exchangers and a metal cost equivalent to the brazed aluminum radiator of conventional primary and secondary surface construction (based on a 1.0 metal cost for the conventional copper radiator). This improvement is achieved with only about 50% of the secondary aluminum fin material required in the brazed aluminum radiator.

The invention will now be described further by way of example with reference to the accompanying drawings, in which:—

Fig. 1 is an end view taken in cross-section of a channel-fin assembly with a seam joint on each channel edge, and the channel-fin formed from a single sheet;

Fig. 2 is an end view taken in cross-section of an alternative channel-fin assembly with the channel and fin elements formed from separate sheets;

Fig. 3 is an end view taken in cross-section of a third embodiment for a channel-fin assembly incorporating one bond joint;

Fig. 4 is an end view taken in cross-section of a fourth embodiment for channel-fin assembly with two fins attached to each channel edge;

Fig. 4A is an isometric view of a channel-fin assembly with a dimpled or folded seam joint and a fin attached to the same channel edge;

Fig. 5 is an isometric view of a channel-fin assembly with slats and slotted apertures arranged in a louvered configuration as the fin surface distortions;

Fig. 5A is an enlarged isometric view of the Fig. 5 assembly;

Fig. 5B is an enlarged cross-sectional view of the Fig. 5 assembly taken along line B—B of the air downstream fin;

Fig. 5C is an enlarged cross-sectional view of the Fig. 5 assembly taken along line C—C of the air upstream fin;

Fig. 5D is an enlarged plan view of the Fig. 5 slatted fin;

Fig. 5E is a cross-sectional view of the Fig. 5 assembly perpendicular to the longitudinal axis X—X along the line A—A;

Fig. 6 is an isometric view of an alternative channel-slatted fin assembly in the form of pleated strips across the fin width as the fin surface distortions;

Fig. 7 is an isometric view of a channel-fin assembly with corrugation as the fin surface distortions, having crests and valleys parallel to the channel longitudinal axis;

Fig. 7A is an end view of two Fig. 7 channel-fin assemblies with corresponding crests and valleys in lateral alignment;

Fig. 8 is an isometric view of a channel-fin assembly with dimples as the fin surface distortions;

Fig. 8A is an end view taken in cross-section of the Fig. 8 channel-dimpled fin assembly;

Fig. 9 is an end view taken in cross-section of a channel-fin assembly having two fins attached to each channel edge and different types of surface distortions on the two fins;

Fig. 10 is an end view taken in cross-section of a two fin per channel edge assembly in which the channel has been longitudinally divided into two separate channels to double fin surface area;

Fig. 11 is an enlarged isometric view of an isostress-type of channel side wall projection portion;

Fig. 11A is an elevation view of a portion of the Fig. 11 channel side wall showing the D and d dimensions;

Fig. 12 is a graph showing the stress vs. surface deflection relationship for different types of channel side wall projection portion contours;

Fig. 13 is an elevation view of a portion of a channel side wall with truncated conical-type wall projection portions;

Figs. 14A—14H comprise a series of schematic isometric views of channel side wall projections having different elevational contours;

Fig. 15 is an isometric view of a two-channel-assembly having louvered fins;

Fig. 15A is an enlarged cross-section view of the Fig. 15 assembly taken along line A—A;

Fig. 15B is an enlarged cross-section view of the Fig. 15 assembly taken in the direction B—B;

Fig. 16 is an isometric view of an automobile radiator employing the Fig. 15 assembly;

Fig. 17 is a graph showing the relationship of heat transfer rate per unit frontal area (H_A)

vs. heat transfer rate per unit weight of metal (H_M) for various types of cross flow automobile radiators;

Figs. 18A, 18B and 18C are graphs showing the relationship of H_A vs. D spacing for the individual components of the Fig. 15 assembly and a similar two fin assembly;

Figs. 19A, 19B and 19C are graphs showing the relationship of H_A vs. H dimension for the individual components of the Fig. 15 assembly and a similar two fin assembly;

Fig. 20 is an isometric view of part of a typical prior art copper automobile radiator of soldered construction;

Fig. 21 shows a diagrammatic elevation view of a wind tunnel used to test automobile radiators;

Fig. 22 is a schematic flowsheet of the automobile radiator test facility;

Fig. 23 is a graph showing capacity (H_A) vs. air volume flow rate for several aluminum automobile radiators tested in the Figs. 21 and 22 facility;

Fig. 24 is an elevation front view of an automobile radiator incorporating the invention;

Figs. 25A, 25B, 25C and 25D are plan views of channel side walls with different wall projection patterns; and

Fig. 26 is a graph showing the change in heat capacity per unit change in weight, for various forms of incremental metal.

Suitable materials for the practice of this invention include aluminum of the 1100 series, aluminum alloy of the 3000 series containing manganese, e.g. Nos. 3003 and 3004; the 600 series containing silicon, e.g. Nos. 6061, 6062 and 6063, and the 5000 series containing chromium, e.g. No. 5052, 5083, 5086, and 5154. The above aluminum alloy sheets clad with a 7000 series aluminum alloy, e.g. No. 7072 containing zinc, are desirable for corrosion resistance. The preferred material is a No. 3003 alloy sheet clad with No. 7072 alloy.

Fig. 1 illustrates a single channel 1 having an elongated cross section bound by side walls 2 and edge walls 3. A fin 4 extends outwardly from each longitudinal seam 5 of channel 1 along the entire length of edge wall 3. In this embodiment the channel-fin assembly is formed of two sheets longitudinally bonded at seams 5. Fins 4 are provided with a multiplicity of surface distortions 6 discussed hereinafter in detail.

In the Fig. 2 channel-fin assembly the channel edges 3 are formed to enclose an edge of fin 4 and seams 5 are formed therebetween. Fig. 2 also illustrates the extension of a fin edge 7 into the channel 1 interior, to be discussed below in detail. The Fig. 1 channel-fin joint is preferred to the Fig. 2 embodiment as the seam length is one-half as long and less metal is required due to double rather than triple metal thickness in the joint area.

The Fig. 3 embodiment illustrates bonding a fin edge directly to the channel edge 3 thereby reducing the required length of the fluid-tight seam in the channel wall, but fabrication of this embodiment is somewhat more complex than Figs. 1 and 2.

In preferred practice at least one fin is attached to both air upstream and air downstream edges 3 of channel 1 as illustrated in Figs. 1—3, and two fins may be attached to each edge wall as illustrated in Fig. 4. Although the fins in Fig. 4 are similar in size to those in Figs. 1 to 3, where the same fin area is required each fin of the double fin arrangement of Fig. 4 need only be one-half as wide as the fins in Figs. 1 to 3. The resulting narrower fin positions all secondary metal surface closer to its juncture with the primary surface channel edge, and reduces metallic heat flow resistance across the fins. Stated otherwise, with a given lower limitation on fin heat conductance the double fin affords twice the secondary surface area as the single fin. Fig. 4 is similar to Fig. 1 in that the channel-fin assembly is formed from two sheets and seam 5 is made by metal fusion. Fig. 4A illustrates the possibility of forming seam 5 by crimping or folding.

Channels 1 and fins 4 have a wall thickness of between 0.003 and 0.015 inch (3—15 mils) preferably between 0.005 and 0.012 inch. Thinner walls than 0.003 inch result in more pronounced undesirable lateral temperature gradients; the edge wall of the channel where fins are attached is chilled to a greater degree and the fins 4 become less effective as a secondary heat transfer surface. This problem is most acute in embodiments such as Figs. 1 and 4 in which the fin is an integral part of the channel, and thereby also exhibits excessive temperature gradients which reduce their effectiveness. If the channel wall thickness exceeds 15 mils the metal thickness begins to occupy an inordinately large fraction of the heat exchanger frontal area. For example, of the center-to-center space between adjacent channels is 0.11 inch, two 15 mil thick channel walls occupy 27% of the total channel area available for fluid flow. Also above 15 mils, metal utilizations (BTU/min.×lb.) become uneconomically small when such thicknesses are also employed for the fins. At greater thicknesses, fin effectiveness is not significantly improved. Channel and fin thicknesses in the range of 0.005 and 0.012 inch represent a preferred balance of these considerations.

As previously indicated each fin is provided with a multiplicity of surface distortions from the fin plane into the gap between adjacent fins of adjacent channels. These surface distortions are closely spaced at intervals S of 0.01—0.2 inches measured normal to the channel longitudinal axis so as to comprise a total distortion area which is at least 40% of the fin surface area, thereby disrupting second fluid flow

across the fin width. These surface distortions substantially reduce the thickness of the second fluid boundary layers relative to the fin surface, as compared to the thickness of second fluid films absent the surface distortions. The surface distortion spacings S should be at least 0.01 inch to effectively disrupt the second fluid film across the fin width in some embodiments and in any event to avoid high stresses, wear and breakage rate of the surface distortion tool. Above S values of 0.2 inch, the length of second fluid flow pass of undistorted metal becomes sufficient to allow the fluid film to thicken excessively. Since the second fluid film is the major resistance to heat transfer, the fin performance is seriously impared. A preferred range of S dimension based on the foregoing considerations is 0.02—0.10 inch. The S dimension is measured in a direction across the fin normal to the longitudinal axis x-x (Fig. 5) of the channel, and functionally is the distance which the second fluid flow is allowed to traverse without termination, interruption or thinning of the fluid film on the fin surface. The total surface distortion area is at least 40% of the fin surface area, also to insure substantial turbulence in and/or disruption of the second fluid film.

The surface distortions generally fall into two categories depending on their mechanism for reducing the second fluid film resistance to heat transfer: surface interruptions and turbulence promoters. The surface interruption type of surface distortion comprises repetitive and closely placed discontinuity in the fin in the direction of second fluid flow across the fin surfaces. A preferred "interruption" type of surface distortion is formed by a louvered fin where slats of the louvre are formed from the fin as tongues to provide apertures in the fins as shown in Fig. 5 wherein the fin metal is slit along closely spaced parallel lines and the metal between the slits thus formed displaced from adjacent metal so that the two edges of a slit are off-set one from the other to form slats. The slats are aligned at an angle to the second fluid flow direction such that the fluid film tending to build up on the fin surface along the flow path is interrupted repeatedly along the fin width.

The "turbulence promoter" type of fin surface distortion comprises a multiplicity of deformations or protrusions in the fin metal such that the metal respectively intrudes and recedes from an otherwise uniform and unobstructed second fluid flow passage across the fin surfaces. The fin itself is not pierced, slit or penetrated at such deformations but instead is bent or dented. Examples of suitable turbulence promoter-type surface distortions include corrugations (Figs. 7 and 7A) and dimplings (Figs. 8 and 8A). As the gas encounters the deformations, it is repeatedly deflected around and over the intrusions of metal. Repetitive local contraction and expansion of the second fluid stream occurs with eddy currents (turbulence) being created particularly on the downstream side of the metal intrusions. As a result, the second fluid film tending to build up is stripped and thinned at many local points of the deformed fin surface. The fin surface distortions may combine the aforementioned surface interruption and turbulence promotion mechanisms for reducing the second fluid film resistance to heat transfer. For example a pattern of pierced dimples in the fins, the dimples acting as turbulence promoters and being pierced to allow a portion of the second fluid to be drawn through the penetration from the concave side to interrupt the second fluid film on the concave side at the mouth of the penetration.

The louvered configuration provides a preferred type of surface distortion of the fins. The slat and elongated aperture form of fin surface distortion can be disposed perpendicular to the longitudinal length of the channel, but, however, when so arranged, the fins would have to be bent at a fin angle γ of about 90° with respect to a plane containing the maximum dimensional width line of, and the longitudinal dimensional length line of the channel, if the slats in the fins are to be aligned to provide a minimum air flow path on the slats for a medium flowing through passages formed between adjacent channels, since such a design would provide maximum heat transfer. The width of a 90° orientated fin will dictate the spacing between the channels. Since compactness is a desirable characteristic in a heat exchanger, such wide spacing should be avoided and the fin should preferably be disposed at an angle γ of less than 90° with respect to the plane containing the maximum dimensional width line, and longitudinal dimensional length line of the channel. On the other extreme, this fin angle γ can be 0° even though the fins would be disposed such that the apertures in the fin would be substantially aligned parallel to the directional flow of a medium between adjacent channels, since in certain respects, this configuration may be desirable from an economical or mechanical viewpoint. Thus the fin angle γ, formed between the plane of the fin and the plane containing the maximum width and longitudinal lines of the channel, can be between about 0° and 90°, but preferably between about 0° and about 60°. If minimum "fin frontal area" is desired, for a given fin bending angle γ, the slot angle α, formed by the longitudinal length line of the channel and the longitudinal length line of the slot, and the slat angle β, formed by the plane of the fin and the plane of the slat member between adjacent apertures, would have to be appropriately chosen. Thus, the designer would obtain substantially maximum area of the slatted aperture orientated normal to the flow of a medium through passages between adjacent channels. "Fin frontal area"

is defined as the area of the projection of the entire array of fins onto a plane normal to the direction of flow of a medium through passages formed between adjacent channels. The slot angle α can vary broadly from 0° to 180° as measured clockwise from the longitudinal axis of the channel to the longitudinal length line of the slot. Preferably the slot angle α should be 90°±45° for most applications since this would provide a sufficient uninterrupted flow path on the fin extending outward from the attached segment points on the channel. The slat angle β can vary between about 15° and about 90° for most applications although an angle between about 30° and about 60° would be preferable since it would provide sufficient slotted apertures which can be obtained through one shot of a die or the like, thus minimizing the manufacturing cost. An angle β of less than about 15° would be insufficient since it would not provide an adequate opening between adjacent slats due to finite material thickness of the fins.

The width of the slats of the louver constructed fins (divided by cos angle α to represent the S distance between adjacent fin surface distortions) should be smaller than about 0.2 inch for most applications, although a slat width of less than 0.10 inch would be desirable. For the lower limit, the slat width should be at least 0.02 inch and preferably at least about 0.03 inch. The smaller the slat width, the smaller the flow path length on the slat for a medium passing through the apertures in a louver constructed fin. Usually finite fin thickness limits the minimum width dimension for the slat of a louver constructed fin.

As specified above, the orientation of the fins and slats can be defined by the angles γ, α, and β. The interrelation of these three angles can be expressed in equation (I) as follows:

$$\sin \theta' = \cos \beta \times \sin \gamma - \cos \gamma \times \sin \beta \times \cos \alpha \quad (I)$$

where θ' is the angle of approach defined as the angle between a first line which is parallel to the plane containing the maximum dimensional width line and the longitudinal dimensional length line of the channel, and perpendicular to the channel's longitudinal length line, and a second line lying in the plane of a slat and in a plane which is normal to the surface of the slat and contains said first line as defined above.

Thus we see that for any one angle γ, α or β, the remaining two angles can vary widely for a specific angle of approach θ' for a particular heat exchange operational mode. By first selecting an angle of approach θ', and then selecting a fin bending angle γ to accommodate a specific array of channels in an overall heat exchanger configuration, the slat angle β and the slot angle α can be substantially varied, and still satisfy Equation I. However, once one of these angles is selected, while maintaining γ and θ' constant, the other angle becomes fixed according to the Equation I. It is thus shown

that γ, α and β can vary widely but they are interrelated in accordance with Equation I which defines the angle of approach which can be selected for a particular application. An angle of approach θ' of about 60° or less would be acceptable for most applications employing the louvred aperture type of fin surface distortion arrangement of this invention, although an angle of approach θ' of about 0° to about 45° is preferable. As can be seen by Equation I, once one of the angles γ, α or β is chosen while keeping the angle of approach θ' constant, then the other two angles cannot be selected independently. Consequently, to provide a desirable fin frontal area for a particular application, the angle of approach θ', fin bending angle γ, the slat angle β and the slot angle α, all of which are related in accordance with Equation I, should be picked so that the plane of each slat will be substantially aligned such that the air flow path across the slats will be substantially minimized.

The slotted fins can be added both fore (front) and aft (rear) of the channel as defined by the direction of a second fluid flow through passages formed between adjacent channels, or otherwise defined as the remote sections of the channel as measured from a plane containing the center points of two adjacent channels and the longitudinal axis of the channel. The width of the fore and aft fins, measured normal to the longitudinal length of the channel, can advantageously be of a different size.

The maximum dimensional width line of the primary-surface heat exchange channel of this slotted fin embodiment can preferably be between about 0.5 inch and 3.0 inches for most applications and the width of the secondary-surface heat exchange slotted fin should be less than about 0.60 inch and preferably wider than 0.10 inch. For automobile radiator applications, the width of the primary-surface heat exchange element of this slotted fin embodiment can vary between about 0.75 inch and about 2.0 inches and the width of the secondary-surface slotted fin can vary from about 0.2 to about 0.5 inches.

Fig. 5 shows a channel 1 with isocompression-type surface distortions 2a, and having a front or fore fin 4a and a rear or aft fin 4b. Fins 4a and 4b extend substantially along the longitudinal edges of channel 1 leaving finless segments at opposite ends of channel 1. The finless segments are designed so that when an array of channels are superimposed in touching relationship, a vertical support or retainer member can be positioned in touching relationship with the edges of said segments as shown in Fig. 16. An enlarged sectional view of channel 1, Fig. 5A, and Fig. 5B, show the various angles γ, α, and β at which fin 4, along with the slats 8 of the louver type arrangement in fin 4, should be oriented so as to provide a multitude of apertures 9 arranged so that the sub-

stantially maximum areas of said apertures 9 are aligned perpendicular to the longitudinal axis x-x of channel 1. For a given set of values of γ and α, maximum aperture area, as viewed from the flow path of an external medium, will correspond to minimum flow path lengths across slats 8. Fin bending angle γ is the angle formed between the plane of the fin 4a, and the plane of the channel containing both the maximum dimensional width line W and the longitudinal dimensional line L of channel 1. To minimize momentum loss in the air flow, the unslotted tip section X' (which is provided for structural strength) should preferably be parallel with the plane of the channel defined above, or to the directional flow of an external medium. The slot angle α is defined as the angle formed between the longitudinal dimensional line L' of the slot, and the longitudinal dimensional line L of channel 1. The slat angle β can best be illustrated from Fig. 5B where it is shown as the angle formed between the plane of the slat 8 and the plane of the overall fin 4. As stated above, the angles γ, α, and β can vary widely depending upon the angle of approach θ' desired. As stated above, and shown in Fig. 5D, the angle of approach θ' is defined as the angle formed between a line A_1 which is parallel to the plane containing lines L and W and perpendicular to the line L, and a line A_2 lying in the plane of a slat and in a plane normal to the plane of the slat and containing line A_1. Slotted aperture area, as viewed from the flow path of an external medium, approaches a maximum only when the angle of approach θ' has low values approaching 0°. Since the heat transfer for a slotted fin is both a function of the width " y " of the slats 8, and the length of the slotted apertures L', it would be advisable to first select the slot angle α to optimize the heat transfer characteristics of the fin. The slat angle β could next be selected based on the material thickness of the fin and on the manufacturing feasibility of the fin as based on mechanical and economical considerations. Fin bending angle γ could then easily be determined for an angle of approach θ' suitable for a particular heat rejection system using Equation 1. As stated previously, fin bending angle γ, slot angle α, and slat angle β, can be varied as long as they satisfy Equation 1 for a selected angle of approach θ'. By determining any two of the angles γ, α and β, and having a desired angle of approach θ', the third angle can be found using Equation 1.

Fig. 5A and 5C show fin bending angle γ', slot angle α' and angle β' for rear or aft fin 4b. Note that the fin bending angle γ' is shown as the opposing angle of fin bending angle γ of fin 4a. This is not necessary and both angles may be positive or negative depending on the direction of α and α', and β and β'. Likewise, slot angle α' and angle β' could be the same or different than angles α and β for fin 4a.

Any artisan can determine when and if it would be desirable to have different angles of γ, α' and β' for the rear fin 4b as opposed to angles γ, α and β for front fin 4a. Preferably, the angles of the front and rear fins including the angle of approach for each fin, should be the same. Economy in the fabrication of the fins alone could dictate the use of the same angles for both front and rear fins.

As an alternative embodiment slats 8 and the intervening slats or apertures 9 may be oriented parallel to the longitudinal length of element 1. The apertures 9 cannot extend substantially along the length of fins 4a and 4b since such a structure would not provide sufficient conductive material extending uninterruptedly outward from the primary-surface material to the tip of each fin. Therefore, slots orientated parallel with the longitudinal length of channel 1 must be regulated in length so as to provide sufficiently wide fin segments extending uninterruptedly outward from the primary-surface material to the fin tip to effectively and efficiently transfer heat from the first fluid in the enclosed channel to the second external of the channel. Depending on the end use application of a heat exchanger employing the finned element of this invention, any artisan can easily determine the length of the slots necessary to provide sufficient conductive paths normal to the longitudinal axis of the heat exchange element. Thus the slots can be disposed anywhere between 0° and 180° with respect to the longitudinal axis of the heat exchanger primary channel provided it yields an angle of approach suitable for a particular end use heat exchange application.

In the Fig. 5 embodiment, the distance S equals slat width divided by cos angle α, as reflecting the second fluid flow across the slat surface. A distance S, which refers to the interval spacing of the fin surface distortion, is shown in Fig. 5B which is a cross section of the channel-fin assembly taken perpendicularly to the longitudinal axis x-x of the channel along line A—A of Fig. 5. The second fluid flows across slats 8 through intervening space 9 in a direction indicated by arrow y-y and thus diagonally traverses the slat surface a distance S. This distance S is greater than the actual slat width by the factor reciprocal cos slot angle α because the slats are inclined α degrees to the plane of longitudinal axis x-x. Stated otherwise, if the slats were aligned with their lengths parallel to axis x-x then distance S would be the slat width, but since the lengths are aligned α degrees to axis x-x S equals the slat width/cos α.

It will also be apparent from Fig. 5 that more than 40% of the fin surface area is deformed to form the louvred configuration, e.g. greater than 90%.

Fig. 6 illustrates another " surface-interruption " type of fin distortion formed by slitting the fin along parallel lines 11 across the fin

width at an angle relative to the channel longitudinal axis x-x and pleating the metal strips between adjacent slits so as to form crests 12 and valleys 13 preferably normal to the angle α. However, the crests 12a and 12b, and the valleys 13a and 13b of adjacent pleated metal strips 14a and 14b are not aligned in the direction normal to angle α, i.e. they are "out-of-phase." Accordingly, adjacent metal strips are repeatedly displaced from one another leaving tent-like apertures 15 extending across fin 4 beneath crests 12 and sloping to valleys 13. As illustrated the second fluid flowing against the fin does not flow lengthwise along pleated strips 14 because the strips are aligned at an angle 90—α to the direction of flow. Accordingly, the gas flows obliquely across the pleated strips 14 from the outer edge to the inner edge, causing repetitive interruptions of the gas film. The distance S between adjacent surface distortions is the crest-to-valley (or valley-to-crest) distance measured normal to the channel longitudinal axis x-x. As illustrated, more than 90% of the fin surface area is distorted into crests 12 and valleys 13. Summarizing, the fin surface distortion of the Fig. 6 embodiment comprises a multiplicity of pleated strips across the fin width and separated by parallel slits, each pleated strip having crests and valleys with apertures formed by the strip edges between said crests and valleys, and with crests and valleys of adjacent pleated strips being non-aligned in the direction normal to said slits.

The fin surface distortions of the Fig. 7 and 7A embodiment comprise a series of corrugations 6 having crests 12 and valleys 13 aligned parallel to the channel longitudinal axis x-x and laterally spaced from each other. The corrugations form surface distortions from the fin plane into the gap between adjacent fins of adjacent channels comprising a total distortion area which is nearly 100% of the fin surface area. The lateral distance S between adjacent crest and valley longitudinal center lines represents the distortion spacing of 0.01—0.2 inches. The corrugations 6 are an example of turbulence promoter-type of surface distortion. The undulations of the metal fin cause acceleration of the second fluid stream against the upstream surface of the crest and cause turbulene on the downstream secondary surface. Both phenomena reduce the thickness of the second fluid film and enhance heat transfer. Preferably, the corrugations 6 of the adjacent fins have corresponding crests and valleys in lateral alignment as illustrated in Fig. 7A so as not to severely restrict the second fluid passage area between adjacent channel-fin assembly. Such restriction would reduce the second fluid flow rate and reduce the effectiveness of the turbulence promoter function of the corrugations. The corrugations 6 are preferably in the sinusoidal shape as illustrated and may be stretched although fin stretching offers both advantages and disadvantages. It produces new surface area for heat exchange contact and this is highly beneficial, but stretching also thins the fin metal and increases its resistance to heat conductance while simultaneous extending the length of the heat flow path. Inasmuch as the gas film heat transfer resistance is usually greater than the metal heat conduction resistance, the generation of new fin area by stretching the metal has an overall beneficial effect. Corrugation lateral spacing S should be less than the fin width in order to effect a plurality of changes in second fluid flow direction across the fin. The ratio of the overall crest-to-valley height F of the corrugations to the lateral spacing S should be between 0.1 and 2.0. If S is less than 0.01 or if F/S is less than 0.1 then the fin performance approaches that of a flat unenhanced fin. If F/S is greater than 2.0 then the corrugations become quite deep relative to their spacing and the friction factor and pressure drop across the fin increase inordinately compared to the increase in heat transfer coefficient.

For maximum turbulence promotion, the corrugations 6 are preferably aligned with the crests and valleys parallel to the channel longitudinal axis as illustrated in Figs. 7 and 7A.

Dimples 6 of Fig. 8 represent another satisfactory turbulence promoter-type fin surface distortion. The dimples are distributed over the fin surface in a pattern such that the second fluid flowing across the fin will repeatedly encounter the dimples. They may be formed in longitudinal rows parallel to the channel 1 longitudinal axis and preferably at uniform intervals (S) across the fin width at the surface distortion spacing of 0.01—0.2 inches. As shown in Fig. 8A the dimples can be formed alternatively concave and convex in the longitudinal rows and adjacent rows can be laterally offset in the lateral direction relative to one another as illustrated in Fig. 8. Also the overall height F from a concave dimple extremity to a convex extremity or to the undeformed plan when dimpling in one direction only is used is at least 0.1 times the center-to-center spacing of adjacent channel-fin assemblies and preferably 0.5 times such spacing, for the same reason hereinbefore discussed in connection with the Fig. 7 corrugation-type surface distortions. The surface distortion spacing S is the shortest distance between adjacent dimples in the lateral direction across the fins. The total distortion area is about 50% of the fin surface as illustrated.

As previously discussed in connection with Fig. 4, it may be advantageous to attach two fins to each edge wall of each channel and thereby position all secondary surface area closer to its juncture with the primary surface wall and reduce metallic heat flow resistance across the fin. The type of surface distortion employed for at least one of a double-fin pair should provide a large fraction of open area for

second fluid flow through the fin, i.e. the "surface interruption" type of distortion as for example illustrated in Figs. 5 and 6. Preferably both of a double-fin pair have this type of surface distortion so that the second fluid stream flows across both sides of both fins and the full secondary surface is effectively utilized. If both fins of a pair were of the "turbulence promoter" type without openings, one fin would shield the other from the gas stream. Fig. 9 illustrates a double-fin embodiment wherein one of the fins 4 has the corrugations 6 of Fig. 7 as the surface distortion. When the two types of fin surface distortions are used in the same heat exchanger, the arrangement must be such that the solid metal fin does not shield the apertured fin. Thus, if the right hand end is the air inlet end, then air deflected into the space between the fin pair 4a can readily escape through the slot apertures of the uppermost slatted fin and continue through the passages between the channels 1. Air approaching the downstream fins 4b contacts the corrugated fin by flowing through the slotted apertures of the lowermost fin.

While doubling the number of fins on each channel edge wall reduces heat flow resistance across the fin, it concentrates a still higher heat transfer duty in the edge wall zone of the primary surface channel. As previously indicated, the edge wall 3 tends to be chilled by the fins and peripherial temperature gradients develop in the channel wall. This metal-chilling effect reduces the effectiveness of the double fin. Fig. 10 illustrates a channel-fin assembly embodiment which alleviates the thermally over-loaded conduction of the edge wall. The Fig. 10 channel 1 embodiment is divided into two separate laterally spaced-apart channel-fin assemblies 1a and 1b, and the linear length of edge wall 3 is doubled for the same channel primary surface area. With four edge walls 3 now available for fin attachment, the heat transfer duty of each edge wall 3 can be materially reduced by spreading out the distribution of the secondary surface fins. When the channels are divided, it is preferred to employ double fins on all channel edges 3 as illustrated in Fig. 10, thereby maximizing heat transfer capacity.

This invention requires that the "wetted area" ratio $(O_C + O_F)/I_T$ of channel outer surface area (O_r) plus fin surface area outside said channels (O_F) to total surface area inside the channels (I_T) be between 1.2 and 4.0. Stated otherwise, the wetted area ratio is the ratio of metal surface area contacted or "wetted" by the second fluid outside the channels, to the metal surface area contacted by the first fluid inside the channel. Usually the fin surface is entirely outside the channel so that the total surface area inside the channel (I_T) is simply the channel inner wall. However, in some instances it may be advantageous to extend the fin inside the channel as illustrated by fin 7

of Fig. 2. Under these circumstances I_T includes the fin surface area inside channel 1. As will be apparent from the foregoing description, the primary surface channels are slender and small, and a wetted area ratio less than 1.2 would require fins too narrow to accommodate and effect the needed surface distortions, i.e. for a channel side wall width of 1 inch the fins would be only 0.1 inch wide. From the heat transfer standpoint such extremely narrow fins do not permit the metal utilization effectiveness of this invention. Wetted area ratios greater than 4.0 correspond to excessive amounts of fin material attached to each of the very limited edge wall areas of the channel and result in ineffective use of fin material on the basis of heat transfer per unit weight of fin metal. This can be best demonstrated with reference to the double-fin embodiment of Fig. 10 with slat-slotted aperture-louvered surface distortions. Consider for example an aluminum heat exchanger with 80 channels per ft. cross section, each 1.00 inch wide with isostress-type side wall projections having wall projection spacings of 0.5 inch normal to the channel longitudinal axis and 0.7 inch parallel to this axis to provide a D dimension of 0.415 inch, H dimension of 0.0545 inch and d dimension of 0.06 inch. At 60 MPH, double fins each only 0.2 inch wide would transfer 576 BTU/min. of a total of 1,041 BTU/min. for the channel-fin assembly. However, on a "per pound of metal" basis the fins would transfer 1081 and 782 BTU/(min.×lb.) for the fore fin and rear fin respectively. The wetted area ratio $(O_C + O_F)/I_T$ for this exchanger is 1.8. If the fin width of the foregoing exchanger were extended from 0.2 inch to 0.5 inch, the fins would transfer 755 BTU/min. of a total of 1172 BTU/min. at 60 MPH. On a "per lb." basis, the fins transfer 580 and 397 BTU/(min.×lb.) for the fore fin and rear fins respectively. Thus on a per fin lb. basis the effectiveness of the fin metal has dropped about 50% of the near-maximum value. The loss of effectiveness is largely due to the chilling effect on the base of the fins. This is the result of thermally overloading the narrow edge wall by means of the very wide double fins. The corresponding wetted area ratio for this exchanger is 3.0. Further widening of fins beyond a ratio of 4.0 would prohibitively reduce the fin heat transfer effectiveness to the point where the use of more channels per foot heat exchanger width (with wetted area ratio below 4.0) is preferable for higher total heat transfer from the standpoint of unit weight of fin metal. The wetted area ratio is preferably between 1.3 and 3.0 as a balance of the foregoing considerations.

This invention also requires primary surface channels having an aspect ratio (or cross-sectional shape factor) of at least 4 and preferably at least 8, wherein the aspect ratio is the

ratio of the length to width of an equivalent rectangle having an area equal to the arithmetic average area of the channel internal cross section and a length equal to the longer internal

5 dimension of the channel cross section. It is necessary to use the equivalent rectangle in defining aspect ratio because the channel cross section is not a regular geometric figure, due to the multiplicity of wall projection portions

10 formed from the channel side wall. Because the channel cross-section varies along the channel longitudinal axis, it is necessary to use the arithmetic average of cross-sections in defining the equivalent rectangle. A satisfactory ap-

15 proximation of the arithmetic average may be based on the maximum cross-section taken at the center of the wall projection portion and the minimum cross-section taken half-way between longitudinally adjacent maximum cross-

20 sections. These areas may be determined by direct measurement from actual cross-sections using a planimeter. Alternatively the arithmetic average may be experimentally determined by measuring the volume of the channel

25 (by filling same with a liquid) and dividing the volume by the channel length. It will be apparent that aspect ratios below 4 mean either reduced channel width relative to channel depth, or increased channel depth relative to

30 width. Reducing the channel width to such an extent reduces the side wall surface area so as to prohibitively reduce the total heat transfer of the heat exchanger. Also, an aspect ratio below 4 increases the probability of plugging

35 due to inability of the first fluid to flow around restrictions in the channel. Moreover such low aspect ratios increase the first fluid velocity and accelerate erosion-corrosion problems in the channel walls. Finally, low aspect ratios

40 increase the difficulty of manifolding the channel ends. If the aspect ratio is reduced below 4 by virtue of increased channel depth relative to channel width, the number of channels per unit exchanger width will be greatly reduced,

45 e.g. below 40 channels per foot cross section (based on 0.8 inch channel width), and the unique compactness of this exchanger (resulting from the other characteristics) would be lost.

50 As previously indicated, each channel is provided with a multiplicity of wall projection portions formed from each side wall being distributed across the side wall surface and extending outwardly therefrom with load-bearing

55 end segments shaped for mating with and abutting against and transferring the load to the outer structural frame, said wall projections portions having a dimensional size and a dimentional relationship thereberween defined

60 by a D dimension of 0.2—1.0 inch, an H dimension of 0.02—0.14 inch and a D/d ratio of 3—18 wherein H is the distance from each load-bearing end segment to the plane of the side wall surface in a direction perpendicular

65 to said plane, D equals the spacing between

the centers of adjacent wall projection portions of a side wall, and d equals the dimension of the ratio 4a/p wherein a equals the area of the load-bearing end segment of the wall-supporting projection and p equals the peri- 70
meter of said load-bearing end segment.

An isostress contoured surface segment A preformed as the channel 1 wall projection portion 2a is shown in Fig. 11 and resembles the contour of a shear-free "soap bubble" 75
membrane. The "soap bubble" membrane shape was closely approached in the formation of projection portion 2a by using a thin, flexible, elastic film of a rubberized material. Members B were utilized to secure the edges 80
of the square segment A to a horizontal plane, defined as the X—Y plane, while the area C, defined as the area contained within the square bound by the B supports, was subject to a hydrostatic pressure to form an isostress con- 85
tour having a height dimension H measured along the Z axis from the X—Y plane at the coordinate intersection of X=0, Y=0. Subjecting a thin structure, having an isostress contour as shown in Fig. 11, to a differential 90
pressure across its wall area C on the convex side thereof will result in imparting substantially pure compression, i.e., isocompression, to the wall void of any appreciable shear or bending forces thereto. Isocompression results 95
in uniform distribution of fiber stress in the cross-sectional area I of wall A parallel to its surface area C as shown by the arrows in Fig. 11. Thus a thin membrane having an isostress contour can withstand greater stress without 100
deforming or rupturing than a non-isostress membrane of identical size and thickness. The formation of isostress-type wall projection portions is described in greater detail in Our British Patent application No. 47238/72. 105
(Serial No. 1,412,442).

When used as the channel 1 wall projection portion 2a, an isostress contoured surface as illustrated in Fig. 11, having a repeatable wall-supporting projection spacing D of between 110
about 0.2 and about 1.0 inch; a D/d ratio between about 3 and about 18, and a sheet or wall thickness between about 0.003 and about 0.015 inch will be quite suitable. As used above and as shown in Figs. 11 and 11A, H 115
equals the maximum height measured perpendicularly from a surface which contains the extremities of the wall-supporting projections (X—Y plane) to the innermost crest of the isostress surface of said element (along the 120
Z axis), D equals the spacing between the center of adjacent wall supporting projections on the surface of said element, and d is the dimension of the ratio a/p whereby a equals the area of the load bearing segment (button) 125
of the wall-supporting projection and p equals the perimeter of said load bearing segment. The load bearing segment is shaped to mate in touching relationship with similar type load bearing segments on wall-supporting projec- 130

tions on a second heat exchange wall.

From the strength standpoint, the allowable deviation from a theoretical isostress contoured surface for automobile radiator applications using 0.008 inch thick aluminum sheet material was investigated by plotting curves of applied pressure (lb/sq. in.) versus surface deflection (inches).

An isostress contoured surface having sixteen wall-supporting projections arranged in a square pattern was stamped on the aluminum sheet. The D spacing between the projected supports was 0.4 inch and the height H was 0.035 inch as shown in Fig. 11A. Pressure was applied to the isostress contoured surface of the aluminum sheet on the convex side of the curvature such as to place the material under compression and the deflection at the center of the diagonals of the square pattern was measured. This data is shown plotted on the graph of Fig. 12. Truncated-conical projections or indentations, as shown in Fig. 13 with cone angles θ of 30° or 45°, and heights H' of 0.035 inch, were likewise stamped onto identical aluminum sheets in the same square pattern and then subjected to the same type pressure versus deflection testing. The data obtained using both the 30° cone and 45° cone projected sheets is also shown plotted as curves on the graph of Fig. 12. The cone angle θ is the acute interior angle measured between the horizontal undeformed surface of the wall adjacent the projected indentation and the substantially straight segment along the sloped side of the conical indentation.

Deflections of the crest of the surface tending to flatten the wall are objectionable and should be minimized even though such deflections may be safely below the buckling point of the material. As noted previously, deflections represent deviations from the ideal soap bubble membrane contour. If the deflections are excessive, the ideal contour cannot be closely approached under service pressure differentials even though allowances are made in the design. Moreover the material is usually stressed in bending and shear as it deflects, and when deflections are excessive the material may experience stresses approaching the yield point in localized area. If such deflections are imposed repeatedly in service, the material may be fatigued and crack after a relatively short service life. Additionally, deflections reduce the available space between the heat exchange walls in the lower pressure passages, and result either in higher fluid pressure drop and in reduced rate of fluid flow. With reference to Fig. 12, it is seen that the isostress contoured wall used in the tests exhibited virtually no deflection at the crest for pressure differentials as high as 35 psi. In contrast, the 45° cone surface deflected severely at low pressure differentials.

In the foregoing tests of the isostress contoured surface, and the 30° and 45° truncated-conical surfaces, the stress in the material was also measured directly by means of strain gauges at 30 psi. differential pressure. The stress was measured on the diagonal at the point where the inclined surface of the conical indentations met the flat, undeformed segment of the material, i.e., in the radius R arc. The following data was taken:

Surface	Stress, psi.
Isostress contour	13,800
30° cone	18,400
45° cone	42,000

The data shows the increase in stress resulting from use of the 30° and 45° cone surfaces over the isostress contour surface. It should be noted that in order to achieve the isostress wall projection portion 2a, it is essential that all the surface area exclusive of the wall projection portions 2a be unrestrictive so as to be free to deflect and therefore be devoid of local mechanical loading.

It should be noted that the tendency to thermally overload the edge walls 3 of the channels with surface distorted fins 4 is a unique consequence of the extremely thin metals employed in the channel wall. The use of thin metals for pressure-containing channels 1 is in turn dependent upon the improved stress distribution afforded by the isostress or frusto-conical contoured wall projections 2a. Due to the thermal overloading tendency of the edge walls 3, the heat transfer contribution of the fins is limited and the high heat transfer capacities demonstrated by this invention would be significantly reduced were it not for the appreciable contribution of the channel walls themselves. In this respect, the wall-supporting projections 2a on the channel side walls 2 also serve as heat transfer enhancements for the primary surface channel. It has been discovered that the isostress and frusto-conical contoured wall-supporting projections 2a increase the overall heat transfer coefficient of the primary surface by about 50% (compared to smooth, flat primary surfaces) at conditions corresponding to normal cruising speeds of automobiles. Typically, under such conditions, the primary walls of a louvered, single-fin exchanger such as Fig. 5 contributes on the order of 60% of the total heat transfer capacity of the heat exchanger, and therefore the 50% enhancement achieved by providing load-supporting wall projection portions 2a in channel side wall 2 is a significant factor. It is evident that the influence of primary side wall heat transfer enhancement would be of little consequence in exchangers with large secondary surface where the " wetted " surface area ratio $(O_C+O_F)/I_T$, air side to water side, is on the order of 8—10. On the other hand, the influence of primary surface heat transfer enhancement is quite important within a range of area ratios between 1.2 and 4.0, as employed in this invention.

Another requirement of this invention is that to maintain the stresses at acceptable levels in both the projection portions and the other portions of the channel walls, the projection portions must have an elevational contour such that the ratio θ/R is between about 4 and 2500 degrees per inch, preferably between about 4 and 100 degrees per inch in an isostress-type wall projection contour. In this ratio, θ is the maximum angle of metal in the projection portion with respect to the base plane of the channel side wall 1 and is measured in a cross-section passing through the projection portion center and perpendicular to the base plane. As used herein base plane is a plane containing the most distant point of the side wall surface from the extremity of the projection end segment and parallel to the flat side wall surface prior to formation of the wall projection portions. For example, in the isostress wall projection of Fig. 11, the base plane passes through point Z and is parallel to a plane containing end segments B, and the cross section through the projection portion center passes through segments B. In a true isostress contoured channel the entire side wall with exception of end segments may be contoured and the intersection of the diagonals between end segments locates the aforementioned most distant point. In the truncated conical-type wall projection of Fig. 13, the surface between surrounding projections is usually flat and such surface constitutes the base plane.

In the aforementioned θ/R ratio, R is the minimum radius of curvature of the sloping walls of the projection portion perpendicular to the base plane, measured outside the projection portion. The radius inside the projection portion at the juncture of the sloping walls and the load-bearing end segment is not used to determine R. The sharpest bend may be in the region where the projection portion begins to rise from the base plane, intermediate this floor region and the projection end segment, or in the vicinity of the end portion itself. The minimum radius of curvature R may be measured readily and conveniently by the well-known optical comparator.

In general, if θ is relatively low, then R (the minimum radius of curvature) can be relatively small. If the maximum angle of metal in the projection portion is steep, then the R should be relatively large. The upper limit of θ/R is based on the truncated conical-type projection. Since, from the maximum stress standpoint it is preferable for θ not to exceed 35 degrees and for the ratio R/D to be at least 0.075, R must be at least 0.015 inch based on a minimum D spacing of 0.2 inch. Accordingly, the θ/R ratio would be about 2333 degrees/inch and the ratio should not exceed about 2500 degrees/inch if excessive stresses are to be avoided.

The lower limit for θ/R of 4 is based on an isostress-type wall projection side wall having minimum projection height H and the largest value of projection spacings D permitted by stresses in the metal. This is because low projection heights H and wide spacings D characterize large low-profile projections having small angles θ and large radii of curvature R. Based on an R dimension of 0.02 inch and a d value of 0.05 inch, the maximum value of D consistent with allowable stress values is about 1.94 and θ is about 9.2 degrees or θ/R of 4.7.

Another example of an isostress-type wall projection of different contour within the aforedefined θ/R range is schematically illustrated in Fig. 14A. The projection height H is the maximum acceptable value of 0.14 inch, the projection spacing is 0.35 inch and the d value is 0.025 inch (consistent with D). Stress is low in a channel side wall with such projections, and a wall thickness of 0.006 inch may be used. Based on the previously mentioned circular cross-section along the diagonal between the isostress-type wall projections, the radius of curvature R is calculated as 0.161 inch and θ as 82 degrees. The ratio θ/R is about 510, well within the range of this invention.

While a θ value approaching or equaling 90 degrees is satifactory in the foregoing example, it should not be assumed that cylindrical or cubic projections formed abruptly from the channel side walls as schematically illustrated in Figs. 14B and 14C respectively, are suitable as the load-supporting wall projection portions. If such projections extend from the side wall through a small radius of curvature R, e.g. 0.015 inch, the value of θ/R would be excessive, e.g. 6000, and the side wall stresses prohibitively high. In order to reduce θ/R for a cylindrical projection to the acceptable upper limit of 2500, the R value at its base would need to be increased to 0.036 inch. This dimension typifies a side wall projection height H useful for this invention, and accordingly the resulting wall projection would lose the abrupt cylindrical contour in the curved metal region joining the base plane and the projection wall. Instead of a cylindrical contour it becomes an isostress-type as schematically illustrated in Fig. 14D.

A frusto-conical type of side wall projection will provide an elevational contour of acceptable θ/R provided that its cone angle θ is low and the radius of curvature at its base is adequate. For example a cone contour with θ of 35 degrees and R of 0.015 inch provides a θ/R ratio of 2333 and is satisfactory. However, a steeper cone contour with θ of 45 degrees and the same radius of curvature, schematically illustrated in Fig. 14E, produces a θ/R ratio of 3000 and is unsuitable by virtue of excessively high stresses. Any side wall projection of conical or other elevational contour,

1,424,689

joining the base metal at a sharp angle is not suitable because as R approaches zero, θ/R approaches infinity.

Fig. 14F schematically represents a squared pyramid type of side wall projection having acceptable θ/R. The sides of the pyramid are curved and may exhibit the general isostress contour. Fig. 14G schematically represents an elongated side wall projection combining features of the Fig. 14F pyramid and the Fig. 14A circular isostress contour, with acceptable θ/R. The end segment of this projection has a rounded contour in the plan view, and the extremities of the segment are also curved so as to exhibit the general isostress contour.

Fig. 14H illustrates an extremely low profile wall projection portion with relatively small θ and relatively large R, i.e. θ/R is less than 4. The elevational contour of metal containing such projections approaches a smooth flat wall; the stresses and deflections are prohibitively high.

Figs. 15, 15A and 15B show two primary surface heat exchange channels 21, 22, having front fins 23 and 24, respectively, and rear fins 25 and 26, respectively, juxaposed in touching relationship with wall projection portions 27 and 28 in contact. Passages 29 in channel elements 21 and 22 define one set of confined first fluid passages independent of, and separate from, a second set of second fluid passages 30 formed between adjacent elements 21 and 22. The first fluid, shown as solid line arrows, can be fed through passages 29 while simultaneously, a second cooler fluid, shown as broken line arrows, can be fed through passages 30 to effectively cause a transfer of heat from the hotter fluid to the cooler fluid without having them intermixed. A portion of second fluid in passages 30 will first pass through slotted apertures 31 and 32 in front fins 23 and 24, respectively, thereby effecting a transfer of the heat which was conducted along the fins 23 and 24, from the primary-surface area 33 and 34, respectively. Likewise, when the second fluid medium leaves passages 30 through slotted apertures 35 and 36 in rear fins 25 and 26, respectively, it again effects a transfer of heat which was conducted along the fins 25 and 26 from the primary-surface area 37 and 38, respectively.

To illustrate an embodiment of the heat exchange elements of this invention, Fig. 16 shows a partial exploded isometric view of an automobile radiator 41 employing such heat exchange elements 42. An array of heat exchange elements 42, having front fins 43 and rear fins 44, and aligned so that their iso-compression-type wall projection portions 45 are arranged such that they extend outward from each wall of a pair and cooperate with similar wall projection portions on the wall of a second pair so as to space apart the walls of a pair to form passages between adjacent channel elements. Member 50 is placed on top

of the array of elements 42 and then support bracket 51 is placed over the assembly along finless channel edge segments as the outer structural frame. This arrangement provides stability for the array of elements 42 in addition to securing proper alignment for elements 42. Support bracket 51 must have an outer plate segment 52 adaptable for securing header 53 thereon, and in addition, it must be capable of providing a leak-tight seal to header 53 and to the channel elements 42 so that in the operational mode, a fluid fed through the elements 42 via header 53 will not leak into the space between adjacent elements 42. A similar type header, not shown, is positioned at the opposite end of elements 42 to provide a compact efficient automobile radiator.

Fig. 17 is a graph comparing the performance of aluminum cross flow heat exchangers of this invention, with the all primary surface-no fin (curve A) and primary surface-smooth finned (curve B) exchangers of British Patent application No. 47238/72 (Serial No. 1,412,442). Curve C is based on the Fig. 5 embodiment having single fins with slats and slotted apertures on each edge wall. Curve D is based on the Fig. 4 embodiment having double fins of the same slats and slotted aperture type on each edge wall. Curve E is based on the Fig. 10 embodiment using two tandem channels (in series with respect to second fluid flow) each having double fins of the same type on each edge wall. Each curve represents an approximate upper and right-hand boundary for the practice of its particular type of channel, or channel-fin combination. It should be understood that the curves and their locations are not intended to be limiting to any embodiment of this invention. The relative positions of the curves do, however, permit comparison of performance between the several types of channels or channel-fin combinations.

The Fig. 17 graph correlates heat transfer rate per unit frontal area (H_A) as the ordinate, with heat transfer rate per unit weight of metal (H_M) as the abscissa. Both H_A and H_M are important criteria for evaluation of automobile radiators: H_A reflects the compactness criteria and H_M reflects the cost criteria. The slope of curves A—E shows that higher H_M tends toward lower H_A, i.e. toward a larger radiator. It is well known that space is scarce in automobile design and construction, and the objective is to obtain high heat transfer with respect to both metal economy and frontal area.

It will be apparent from Fig. 17 that the present invention offers substantial improvement in both respects, as compared to an all-primary surface exchanger (curve A) or an exchanger of similar type channels provided with smooth, unenhanced fins (curve B). By way of example, for H_M of 450 BTU/min.× lb. neither the curve A or curve B exchangers are suitable. That is, in order to reach such heat transfer rate per unit, weight, the heat

transfer rate per unit frontal area would be far below the range of the ordinate scale (below 600 BTU/min.×ft²). In contrast, the single fin curve C exchanger of this invention could readily obtain a H_M of 450 BTU/min.×lb. and would achieve a corresponding H_A of over 1100 BTU/min.×ft². Alternatively, the same H_M value of 450 BTU/min.×lb may be achieved with two fins per edge wall in a more compact curve D exchanger and obtain over 1300 BTU/min.×ft². As a further choice the primary surface may be divided among twice the number of narrower channels as illustrated in Fig. 10, to provide the edge wall length for fin attachment. This curve E exchanger is capable of transferring over 1500 BTU/min.×ft² frontal area at H_M of 450 BTU/min.×lb. and is even more compact than the curve D embodiment.

The advantage of the present invention in terms of metal cost may be quantified by comparing H_M values at a required H_A value of 1000 BTU/min.×ft². The corresponding H_M values for curves A, B, C, D and E designs are as follows: <300, 360, 485, 550 and >550 BTU/min.×lb., respectively. The Fig. 17 comparisons are summarized in Table A.

TABLE A

Type of Heat Exchanger	H_A at H_M = .450	H_M at H_A = 1000
All primary surface (curve A)	<600	<300
Smooth fins (curve B)	<600	360
Single fins with slats and slot apertures (curve C)	1160	485
Double fins with slats and slot apertures (curve D)	1320	550
Narrow primary surface, double fins with slats and slot apertures (curve E)	1550	>550

As previously indicated, the wall projection portions of the primary side walls have a D dimension of 0.2—1.0 inch, and H dimension of 0.02—0.14 inch, and a D/d ratio of 3—18. The reasons for these parameters will now be explained in connection with the graphs of Figs. 18 and 19.

The cross flow exchanger of this invention must permit adequate flow of second fluid through the space between adjacent primary surface channels and around the surface distorted metal fins, to insure sufficient fluid flow conductance. The primary surface channels are preferably stacked sufficiently closely to provide 40—150 channels per foot of heat exchanger cross-section, and this corresponds to a center-to-center spacing of 0.08—0.3 inch. A portion of this center-to-center dimension is occupied by the first fluid-transporting channels and another portion by the channel walls, so that the second fluid passages are quite thin and narrow. Moreover the wall projection portions from the primary surface side wall, needed for wall support, intrude into and further diminish the available space for second fluid flow between the channels. The flow resistance encountered by air as the second fluid in the passage between the channels represents a large fraction of the total air flow resistance through a radiator-type heat exchanger, the balance being due to the surface distortion-containing fins. For example, in the slat-slotted aperture louvered fin embodiment of Fig. 5, the air pressure drop between the channels may be over 10 times that through the fins.

Whereas the wall projection portions substantially increase the overall heat transfer coefficient of the primary surface channel, they nevertheless also exert the adverse effect of increasing flow resistance in the second fluid passage between adjacent channels. The beneficial heat transfer enhancement effect is greater than the adverse flow resistance effect insofar as economy of the primary surface channels is concerned. However, a decrease in the second fluid flow conductance (or increase in flow resistance) across the passage exerts an adverse effect on fin performance because it reduces the second fluid flow rate over the fin, in-

creases the second fluid film resistance on the fin surfaces, and reduces the ΔT driving force for heat transfer between the surface distorted fins and the second fluid.

The channel side wall projection portion dimensions (height H, spacing D and ratio D/d) are important factors in determining the second fluid flow conductance in the passage between primary surface adjacent channels, i.e. this conductance is improved with relatively large values for these factors. However, H and D are desirably small dimensions from the standpoint of the primary surface alone, for reasons set forth in previously referenced patent application No. 47238/72 (Serial No. 1,412,442). In brief, H must be small in order to obtain a large number of channels per unit heat exchanger width (cross section) and hence to obtain a large primary surface area. The side wall projection spacing D has a pronounced effect upon the channel side wall stress level, and must be small when thin materials are employed.

It has been discovered that the effect of changes in D dimension on heat transfer performance of the surface distorted fins tends to be opposite to their effect on the primary surface channel. Reducing the D dimension toward relatively small value tends to eventually increase the heat transfer contribution of the primary surface channel (due to the greater enhancement effect of more wall projection portions) but decrease the fin contribution to overall heat transfer, other factors remaining constant. The decrease in fin contribution to heat transfer is due in part to the "choking" effect of the smaller spacial dimensions of the second fluid flow passage between adjacent primary surface channels. Increasing the D dimension toward relatively high values (other factors remaining constant) tends to eventually produce a similar trend in the heat transfer contributions of the primary surface channel and distorted secondary fin surface. That is, it tends to increase the heat transfer contribution of the primary surface channel and to decrease the contribution of the fins. This effect at large D dimension is not clearly understood but is believed to be due in part to a sustained high heat transfer coefficient in the secondary fluid passage between primary surface channels where the major part of the second fluid pressure drop occurs, and where the larger flow of second fluid (e.g. cool air) increases the ΔT driving force between the second fluid and the channel walls.

The foregoing opposite heat transfer characteristics of the primary surface channel and the distorted secondary fin surface in terms of primary surface distortion spacing D have been found to exhibit minima in the heat transfer per unit frontal area (H_A) vs. D spacing curves for the primary surface channels (curve B) and maxima in such curves for the fins (curves C and D). These curves are illustrated in Figs. 18A, 18B and 18C for the Fig. 5 single louvered fin embodiment. More particularly, the solid curves A—D are based on 0.8 inch wide aluminum alloy channels spaced 0.133 inch center-to-center, with 0.3 inch wide front and rear single aluminum fins provided with 0.035 inch wide slats having the following characteristics: $\theta' = 0°$, $\beta = 74°$, $\gamma = 56°$, and $\alpha = 65°$. The dashed-line curves A'—D' are based on the same dimensional specifications for the aluminum channels and louvered fins, but with two such fins on each channel edge wall as illustrated in Fig. 10. The approximate wall projection portion density (projections per in² side wall surface area) are also shown on the abscissa for corresponding values of D. Curve E shows metal stress in the channel walls at 15 psi. internal pressure, when the channel side walls are formed with the isostress wall projection portion substantially as shown in Fig. 11. The ordinate H_A is in units of BTU/min.$\times$ft² and the scale is numerically identical to values of metal stress (lbs./in²).

Figs. 18A, 18B and 18C depict H_A vs. D and projection density relationships for cross flow aluminum alloy heat exchangers fabricated of 0.006, 0.008, and 0.015 inch aluminum respectively. The curves show the heat transfer achieved by the total of all components (curve A), the primary surface channel (curve B), the front fin (curve C) and the rear fin (curve D). The design of cross flow heat exchangers represented by the Fig. 18A, 18B and 18C curves is in part based on a maximum fiber stress dependent upon the probable mode of failure and the desired safety factor for stress. With the isostress or frusto-conical contour wall projections, failure of aluminum alloy channels will normally occur in the vicinity of 16,000 psi. Applying a stress factor of safety of 2 or based on 8000 psi., it is evident that strength considerations impose an upper limit for D spacing of about 0.85 inch for the thickest metal, i.e. 0.015 inch thick aluminum alloy sheet per Fig. 18C. However, Figs. 18A, 18B and 18C are based on a channel density of about 90 channels per foot of heat exchanger cross-section. For lower channel densities also suitable for practice of this invention, the stress for the same range of D spacings is reduced and falls below an acceptable value of 8000 psi. at channel densities of about 40—60 and D spacings up to 1 inch. For high heat transfer rate per unit weight of metal (H_M), it is desirable to design the heat exchanger to operate at relatively high allowable stresses. It was surprising to discover that the D spacing range of 0.2—1.0 was suitable from this standpoint and also from the standpoint of high overall heat transfer rates (H_A) as evidenced by curves A and A'. Another reason for the D spacing upper limit of 1.0 inch is that higher spacing make it difficult if not impossible to locate two wall projections across

the channel width, and this is desirable from the standpoint of channel load distribution through the load-bearing end segments of the wall projections.

5.   As the D spacing is decreased toward low values, excessive stress is no longer a limiting factor, but the very low metal stress represented by curve E indicates an uneconomical use of metal, i.e. low values for heat transfer

10   rate per unit weight of metal (H_{w}). Low D spacings below 0.2 inch undesirably increase the second fluid pressure drop and increase the probability of plugging and increased restriction of second fluid flow in the space

15   between adjacent channels. Finally, for a given wall projection height H, D spacings below 0.2 inch increase the difficulty of forming the wall projection portions and the likelihood of breakage. For these reasons, the D spacing of

20   the primary surface wall projections should be at least 0.2 inch in the practice of this invention, the preferred range being 0.3—0.85 inch. A preferred range of O/d ratio is 6—14.

Curves E of Figs. 18A, B, C associating

25   stress with wall projection portion D spacings are not to be quantitatively applied to all possible geometric patterns of projection locations on the channel side walls, but only to simple and regular projection patterns with triangular

30   units not greatly varying from equilateral triangles. As a guideline, the use of stress curves E should be limited to wall projection patterns whose triangular units are characterized by $D_{min}/D_{max} \geq 0.8$, where D_{min} = the smaller of

35   D_1 and D_2, and D_{max} = the larger of D_1 and D_2. Complex patterns such as Fig. 25D discussed hereinafter or those in which D_{min}/D_{max} exceeds 0.8 should be analyzed experimentally to determine the relationships of

40   maximum allowable stress and/or heat transfer capacity versus wall projection D spacings.

Fig. 19A, 19B and 19C illustrate the aforedescribed relationship between the primary surface wall projection height H as the abscissa

45   vs. heat transfer per unit time and frontal area H_A as the ordinate. The approximate number of channels per foot of heat exchanger crosssection is shown on the abscissa for corresponding values of H. However for a given value of

50   H, the primary surface channel density may vary slightly depending on the overall depth specified for the channel. Also as in Figs. 18A, B, C the ordinate scale is numerically identical to values of metal stress (lbs./in²). However

55   the wall projection spacings are held constant at 0.5 inch in the direction normal to the channel longitudinal axis and 0.6 inch in the direction of the channel longitudinal axis, i.e. a D spacing of 0.56 inches according to the

60   foregoing equation. The other dimensions (channel width, d and fin width) and the geometrical characteristics of the slat-slotted aperture-louvered fins are the same as in Figs. 18A, B, C.

65   Figs. 19A, 19B and 19C are based on cross

flow aluminum alloy heat exchangers fabricated from 0.006, 0.008 and 0.015 inch thick metal respectively, and curves A, B, C, D and E as well as curves A', B', C', and D' relate to the same constructions so identified in Figs. 18A,   70 18B and 18C. The dotted curves F indicate H_w or heat transfer rate per unit time per unit total weight of heat transfer metal (BTU/min. ×lb.), and may be read directly from the ordinate scale.   75

It should be understood that whereas varying D as in Figs. 18A, B, C does not alter the amount of metal used per unit of heat exchanger frontal area, varying H as in Figs. 19A, B, C changes the metal weight significantly.   80 As H is reduced, the channels become thinner and more primary surface channels are employed per foot width of cross-flow heat exchanger. It is evident from Figs. 19A, B, C that the total heat transfer curves A and A'   85 reach maxima at wall projection height H values of about 0.02 inch, corresponding to about 150 channels per foot of heat exchanger width. Below H values of 0.02 inch, the heat transfer performance of the rear fin is seriously   90 impaired, i.e. curve D slopes sharply downward. This effect is attributed to high second fluid passage flow resistance as the spacing between adjacent channels becomes narrower. Further addition of heat transfer surface per   95 unit frontal area is fully offset by a reduction in heat transfer effectiveness of such metal. The decreasing heat transfer effectiveness of the metal per unit weight is indicated by the downward slope of curves F. Curves E show that   100 stress increases at lower values of H. This factor must be appropriately taken into account in designing the cross-flow heat exchanger, but in actual practice is usually not limiting on H. For example, if the wall projection spacing D   105 (held constant in Figs. 19A, B, C) were reduced for lower values of H, the stress could be further suppressed so that wall projection heights down to 0.02 inch can be easily attained without approaching the buckling limit   110 of the channel wall. For the foregoing reasons, the channel side wall projections should have H values of at least 0.02 inch in the practice of this invention.

As the side wall projection portion height   115 H is progressively increased to relatively high values, the heat transfer per unit frontal area eventually declines for all components of the heat exchanger, i.e. the channels of curve B and the front and rear surface distorted fins   120 of curves C and D. Accordingly, for a given heat transfer load, the cross flow exchanger must become larger and less compact as demonstrated by the downward slope of curve A. However, the curve F heat transfer per   125 unit weight continues to increase and reaches maximum value at a wall projection height H of about 0.14 inch (40 channels/foot of exchanger width). Beyond this point further expansion of the exchanger by increasing H   130

1,424,689

achieves no further improvement in metal utilization and unnecessarily enlarges the exchanger. The decline of performance at higher values of H is believed due to channels and second fluid passages of excessive depth, reduced fluid turbulence and therefore lower heat transfer coefficients. In view of the substantial downward slope of the total heat transfer per unit frontal area curve A and the maximum of the total heat transfer per unit metal cost curve F at about 0.14 inch, the wall projection height H of the instant cross flow heat exchanger should not exceed this value.

The preferred range for H values is 0.025—0.1 inch.

The advantages of this invention are demonstrated by the following examples:

EXAMPLE 1.

Three aluminum alloy one-square-foot heat exchangers with isostress-type wall projection portions, two finless and one finned, were constructed from 0.008 inch thick material as shown in Fig. 15 with the following dimensional parameters in inches:

TABLE B

Number	D	D/d	H	θ/R	Aspect Ratio	Wetted Wall Area Ratio
1	0.405	4.7	0.035	20.6	25.1	1
2	0.63	10.5	0.035	10.1	32.7	1
3	0.41	6.8	0.035	15.6	61.1	1.7

Three conventional type copper radiators, typified by the radiator shown in Fig. 20 and modified to one square-foot heat exchange frontal area size were also provided, and all were tested in a wind tunnel shown schematically in Fig. 21. The prime function of the test was to measure and compare the heat transfer capacity of the different type heat exchangers. This was accomplished by pumping heated coolant through the test radiators at a fixed rate as shown in Fig. 22 while varying the air flow rate as shown in Fig. 21. As shown in Fig. 22, steam was fed from a supply source (not shown) through a feedback control valve 80 and through a 0-to-30 psi. gauge 81. The steam was controlled by valve 82, parallel coupled to a finer adjustment valve 83, before being fed into a water heater tank 84. The pressure in the tank 84 was measured by a 0—60 psi. gauge 85. The water output from the tank 84 was fed into a test radiator 86 and upon exiting from the radiator 86, the water was pumped by motor 87 via parallel coupled control valve 88 and series control valve 89 back into the heater tank 84. A water meter 90 was connected downstream of the pump 87 so as to measure the water flow through the radiator 86. Steam condensate in the tank 84 was discharged into a receptacle, not shown. The feed rate of the heated coolant through the radiator was thus controlled at all times, and although not shown, temperature measuring device were used to record the temperature of the water into and out of the radiator.

The test schematic of Fig. 21 shows a wind tunnel used to regulate the rate and temperature of an air flow through the passages formed between adjacent heat exchange elements in the radiators being tested. Air entering the tunnel was first passed through a calibrated orifice 60, which measured the air volume flow into a four cubic foot plenum chamber, and then fed through flow straightening screens 62 into a tapered adapter section 63. The adapter section 63 was provided to effect a smooth transition in the air flow between the plenum chamber 62 and a one square foot wind tunnel duct 64 coupled to a test radiator 65. A blower (not shown) was positioned downstream of the radiator for controlling the air flow through the radiator. The heated air from a radiator 65 was either exhausted via damper 66 or recirculated into the test room via damper 67 so as to provide a degree of temperature control within the room. To reduce the air flow rate through the radiator, control damper 68 was coupled downstream of the exiting air flow from radiator 65. The tapered adapter section 63 and the flow straightening screens 62 were successful in keeping velocity variation through the test radiator 65 at a minimum. Velocity profiles and pilot tube readings made over the frontal area of different test radiator 65 indicated that air velocity variation for all the radiators tested was within ±5%. One 0-to-2 inch manometer 69, and two 0-to-4 inch manometers 70 were positioned as shown in the test circuit and used to measure the air pressure drop. Two grids, 72 and 73, containing four thermocouples, each of which was placed in the

center of one quarter of the flow passage area of the radiator 65, measured the average inlet and exit air temperature through test radiator 65. A Brown multipoint chart recorder (not shown) and a Rubicon potentiometer (now shown) were coupled to the grids and recorded the thermocouple readings. Thus, an accurate test circuit was provided for measuring the heat transfer capacity of the test radiators.

Test radiator number 1 with isocompression type wall projection portions, similar to that shown in Fig. 15 except it was finless, was fabricated by pressing the "right" and "left" channel halves of aluminum between male and female epoxy isocompression dies prepared as described in my above-identified patent British Patent application No. 47238/72 (Serial No. 1,412,442). The isocompression impressed channel halves were then trimmed and folded longitudinally on the edge, whereupon they were degreased, acid cleaned and treated with a surface pretreatment agent known as Alodine, followed by a water rinse. Alodine is a trade mark of Amchem Products Inc.

After drying, an epoxy based adhesive known as Resin Type EA—914, manufactured by the Hysol Division of Dexter Corporation, California, was applied to the 13-inch long folded edge on each channel half, and mating channel halves were then joined to form a 1.625 inch wide channel. The channel was then placed in a fixture and rolled seam tight. After removing the excess adhesive from the channel, the adhesive in the seam was oven cured. Thereafter the channel ends were expanded and an adhesive was applied to each of the wall projection portions and to the channel wall ends. Temporary inserts for wall support were inserted at the channel ends and an array of ten channels were clamped in touching relationship in a fixture and then the adhesive was oven cured. Thereafter the array of channels were again cleaned as specified above and then assembled into a header as shown in Fig. 16. Once again adhesive was used to seal the channels to the header thus providing a test radiator.

Test radiator number 2 (also provided with isocompression-type wall projection portions) was prepared similar to the above except that the projection portions were not adhesively secured together. The width of the channels measured 1.9 inches, and the length was 13 inches.

Test radiator number 3 (also provided with isocompression-type wall projection portions) was prepared similar to test radiator number 2 except that the seams were welded, and slat-slotted aperture fins were disposed on the fore and aft longitudinal edges of the channel, as shown in Fig. 15. The overall width of the channel and fins measured 1.7 inches and the unbent fins measured 0.2 inch and 0.5 inch at the fore and aft longitudinal edges. The length of the channel measured 13 inches. The slot

angles α and α' measured 45°, the slat angle β and β' measured 40° and the bending angles γ and γ' varied for six fin configurations as follows:

TEST RADIATOR 3.

Type 1 Short and long fin unbent, short fin forward

Type 2 Short fin bent 30°, long fin unbent, short fin forward

Type 3 Short fin bent 30°, long fin unbent, long fin forward

Type 4 Short fin bent 30°, long fin bent 15°, short fin forward

Type 5 Short fin bent 30°, long fin bent 30°, short fin forward

Type 6 Short fin bent 30°, long fin bent 30°, long fin forward

The slat width was 0.035 inch so that S equals $0.035/\cos \alpha = 0.049$ inch.

Three similar type conventional automobile radiators, test numbers 4, 5 and 6, typical copper core consisting of brass tubes soldered to thin copper fins, except for varying fin and tankage configurations, were modified to one square foot heat exchange frontal area by cutting the core and reinstalling a shortened header and tank. Thus all test radiators were designed to yield one square foot heat exchange frontal area. The surface distorted finned iso-stress wall projection test radiator cost subsequently less to make than the conventional copper-brass test radiators because in the former, the cost of the base metal material was less per pound than the base metal material of the latter.

The nominal test conditions for the various radiators are shown in Table C. Of the conventional radiators tested, test radiator 4 was found to be superior on a heat transfer per unit of air horsepower basis. Thus radiator 4 was compared to test radiators 1, 2 and 3. In this radiator the copper fins were 0.475 inch wide, 0.003 inch thick, and the fin spacing was 12.4 fins/inch measured in a direction parallel to the channel longitudinal axis. The channel external width and depth were 0.485 inch and 0.090 inch, respectively. There were twenty-one channels spaced across the 1 foot radiator with a 0.475 inch gap (the fin width) between adjacent channels.

Fig. 23 shows a plot of capacity vs. air volume flow rate for the test radiators 1 through 4. The conditions for the plot was 100° F. average coolant fluid to inlet air temperature difference, using a 50% by volume ethylene glycol-50% water coolant at a flow rate of between 14—17 gallons per minute. As illustrated in Fig. 23, radiator 3 Type 5 had a higher capacity for the same air volume of flow rate than the best conventional type radiator, radiator 4.

TABLE C

Test No.	Number of Runs	Temperature		Flow Rate	
		Inlet Air °F.	Inlet Water °F.	Air CFM	Water CFM
4	8	90	215	600—2700	15
	8	90	240	450—1650	17
5	8	90	180	600—1700	17
	8	90	190	600—2000	17
	8	90	200	600—1900	14
	8	90	210	600—2100	17
	8	75	185	600—2000	14
6	8	90	210	650—2500	17
1	16	90	210	400—1250	17
2	16	90	210	400—2000	17
3					
Type 1	8	75	185	600—1800	14
Type 2	8	75	185	600—1800	14
Type 3	8	75	185	600—2000	14
Type 4	8	75	185	600—2000	14
Type 5	8	75	185	600—2000	14
Type 6	8	80	185	600—2050	14

The result of this test proved that the surface distorted finned isostress wall projection aluminum radiator of this invention will perform comparably to the best conventional automobile radiator and cost substantially less to make because of optimum metal utilization. Thus this invention provides economical, compact, light-weight, finned heat exchange channel elements that can be assembled into an efficient heat exchanger for various applications.

Calculations based on the experimental data of the test for radiator 3 in its various configurations revealed the following:

TABLE D

Heat Transfer Coefficient, BTU/Ft² °F. Hr.

	Low Speed (600 FPM Approach Velocity)		High Speed (1200 FPM Approach Velocity)	
	Primary Surface	Secondary Surface	Primary Surface	Secondary Surface
Type 1	20.2	13.7	30.6	20.6
Type 2	20.3	23.0	30.5	39.3
Type 3	20.2	18.6	30.7	34.0
Type 4	20.2	27.0	30.5	47.0
Type 5	20.4	31.5	30.3	53.0
Type 6	20.4	30.5	30.6	52.0

Thus a radiator having a front fin with the same bend angle γ of about 30° as the rear fin and exemplified by Type 5, was preferred for an automobile radiator using the specific type heat exchange channel element tested.

A radiator similar to that shown in Fig. 5 and constructed as specified for test Radiator 3 Type 5 was installed in an automobile and when subjected to local driving conditions, the radiator performed admirably.

EXAMPLE 2.

The effect of providing the previously defined surface distortions to secondary fins attached to the primary surface channels with wall projection portions, is also illustrated by the following example. A heat exchanger contains 80 channels in a width of 12 inches and a height of 12 inches, and each channel is provided with a single fin 0.459 inch wide along the front and the rear edges. The channels are 0.800 inch deep (long external dimension of the cross-section) and their flat sidewalls are formed with the isostress-type wall projection portions 0.06 inch high (H dimension), spaced 0.6 inch vertically and 0.5 inch horizontally (D dimension of 0.39 inch) and having 0.060 inch tip diameter (d dimension). All metal is 0.008 inch thick aluminum. The channels are manifolded top and bottom, and 40% by volume ethylene glycol-in-water at 190° F. is pumped through the channel side at 35 gpm. Air at 90° F. and essentially atmospheric pressure is blown between the channels in cross-flow direction at about 1900 cu. ft. per minute. In one case, the fins are

smooth, straight and continuous and are aligned on the long axis of the channel cross-section. In another case, the fins are the slat-slotted aperture single louvered type as illustrated in Figs. 5 and 15. For both front and rear fins, $\alpha=65°$, $\beta=74°$, $\gamma=56°$, and the slat width is 0.035 inch. With these conditions, the heat transfer coefficients for the straight smooth fins were found to be about 9 BTU/hr.$\times$ft²$\times$° F. Under the same conditions, the louvered fins provided a heat transfer coefficient of about 53 BTU/hr.$\times$ft²$\times$° F. for both front and rear fins. The factor of improvement under these conditions is about 5.9.

EXAMPLE 3.

The effect of providing slat-slotted aperture louvered fins to channels having isostress-type wall projection portions is further illustrated by comparative data based on several cross flow heat exchangers: Type A is all primary surface with 1.35 inch deep channels, Type B has 0.8 inch deep channels and 0.3 inch wide single front fins and 0.3 wide single rear fins, Type C has 0.8 inch deep channels and 0.3 inch wide double front fins and 0.3 inch wide double rear fins, Type D has 0.5 inch deep channels and 0.4 inch wide double front fins and 0.35 inch wide double rear fins (see Fig. 10) and double channels. The other fin dimensions and angles are the same as described in Example 2, and the double fins are arranged as in Fig. 10. The remaining important geometric parameters for the four types of heat exchangers formed from 0.008 inch thick aluminum alloy sheet are as follows:

1,424,689

Parameter	A	B	C	D
D (inches)	0.39	0.39	0.39	0.46
D/d	7.1	6.5	6.5	7.7
S (inches)	none	0.083	0.083	0.083
Aspect ratio	22.5	15.5	13.9	8.0
$(0_C + 0_F)/I_T$	1	1.75	2.5	4.0
Channels/ft.	99	100	90	79.5

These four types of heat exchangers may be compared in terms of the individual components of H_A, heat transfer per minute per unit frontal area in the automobile radiator cooling system of Example 2 at different speeds as follows:

Heat Exchanger Type and Component	Heat Transfer per Minute per Unit Frontal Area (Btu/min × ft²) Miles per Hour			
	0	30	60	90
A — channel	357	565	889	1193
B — channel	209	322	512	688
front fin	105	191	305	394
rear fin	61	128	221	297
total	375	640	1037	1379
C — channel	158	252	408	556
front fins	169	303	478	615
rear fins	94	195	334	451
total	420	750	1221	1621

Heat Exchanger Type and Component	Heat Transfer per Minute per Unit Frontal Area (Btu/min × ft²) Miles per Hour			
	0	30	60	90
D — front channel	62	100	164	224
front fins	170	303	459	578
rear fins	103	209	346	456
sub-total	335	612	969	1258
rear channel	32	60	109	159
front fins	88	182	306	409
rear fins	53	125	231	323
sub-total	173	367	646	891
Grand Total	508	979	1615	2149

The H_A present improvement of type B, C and D heat exchangers over Type A are substantial at all speeds with best results achieved in Type D as follows: 0 mph = 42%, 30 mph = 73%, 60 mph = 81%, and 90 mph = 80%.

Fig. 24 illustrates an automobile radiator embodying the cross flow heat exchanger of the present invention, including finned channel

sandwich assembly 91 supported by outer side frame 92. The first fluid channels extend longitudinally top-to-bottom and are joined at their top ends by top tank manifold 93 and at their bottom ends by bottom tank manifold 94. First fluid is introduced through top filling connection 95. Second fluid is circulated across the first fluid channels and normal to the Fig. 24 plane by a fan located behind the radiator (not illustrated). In operation, the hot first fluid (usually water-ethylene glycol mixture) is introduced through a hose connection (not illustrated) in the back side of top tank manifold 93 and thence to the channels for downward flow therethrough in heat exchange with the cooler second fluir (air) flowing across the channels. The cooled first fluid is discharged from the channel bottom ends into bottom tank manifold 94 and thence through hose connection 96.

As previously indicated, D equals the effective spacing between the centers of adjacent wall projection portions of a channel side wall as determined by the following formula reflecting the fact that stresses in the projection-supported wall are approximately proportional to the third power of projection spacing:

$$D = 3\sqrt{\dfrac{D_1{}^3 + D_2{}^3}{2}}$$

wherein

D_1 = shortest distance between two adjacent wall projection centers in any triangular unit of the projection pattern on the side wall,

D_2 = perpendicular distance from a straight line extending through said two adjacent wall projection centers to the center of the third wall projection of the triangular unit, and

triangular unit = a triangle having a wall projection center only at each of its apexes, with each side of the triangle extending between wall projection centers without transversing a shorter line segment interconnecting other projection centers.

When the wall projection portions are equally spaced and disposed in a square pattern over the channel side wall, the dimension D is the center-to-center distance between the closest adjacent projections and D_1 equals D_2. Thus in Fig. 11, D is the distance along the side of the square element rather than across the diagonal thereof. However, when the projection pattern is other than square and the spacings are not equal, then D_1 and D_2 are different and the effective D is not a direct measurement on the channel side wall.

Figs. 25A to D illustrate four feasible patterns of projections with unequal spacings and shows the method used to determine D_1 and D_2 from the foregoing equation. Each drawing 25A, B, C and D, represents the plan view of the side wall of a channel, and fins have been omitted for simplicity. Fig. 25A shows a recti-linear pattern of projections and the triangular unit is typified by triangle abc having a wall projection center at each apex. The closest spacing between wall projection centers of the triangle is side cb which becomes D_1. The perpendicular distance from a line through c and b to the third apex "a" is side $\overline{ca}$ of the triangle and therefore $\overline{ca}$ becomes D_2. Because of the simplicity of the pattern, only one triangular unit is present.

Fig. 25B illustrates an off-set or diamond pattern of projections. One triangular unit is represented by triangle abc and as illustrated, sides $\overline{bc}$ and $\overline{ca}$ are equal and are the shortest distance between wall projection centers of the triangle, thus $\overline{bc}$ (or $\overline{ca}$) becomes D_1 and the perpendicular from that side through the third apex becomes D_2. Triangle def is a second triangular unit found in the pattern, and as illustrated, sides $\overline{de}$ and $\overline{ef}$ are equal and are the shortest distance between projection centers of the triangle, thus side $\overline{ef}$ (or side $\overline{de}$) becomes D_1 and the perpendicular to a line containing such shortest side and passing through the third apex of the triangle becomes D_2. It should be noted that triangle ghi may also be drawn between wall projection centers but does not meet the requirements of a triangular unit inasmuch as side $\overline{gi}$ transverses both line segments $\overline{eh}$ and $\overline{fh}$ which interconnect other projection centers and are shorter than $\overline{gi}$. The D dimension for this projection pattern would be determined by calculating the values for each of triangles abc and def, and selecting the larger value as limiting from the heat transfer and stress standpoints.

Fig. 25C illustrates off-set vertical rows of projections and the single triangular unit which it contains is typified by triangle abc. As illustrated, side $\overline{ca}$ is the shortest distance between projection centers and becomes D_1. The perpendicular to side $\overline{ca}$ passing through the third projection center at "b" becomes D_2. Triangle def does not meet the requirements of a triangular unit because side $\overline{df}$ transverses a shorter line segment $\overline{ge}$ interconnecting other projection centers.

The foregoing pattern arrangements of Figs. 25A, B and C are quite simple and regular in nature. In some cases, it may be desirable to employ a more complex pattern such as that shown in Fig. 25D. The projection arrangement of Fig. 25D positions a relatively large number of projections near the edge wall of the channel, thereby lending additional support to the edge wall area. The pattern illustrated consists of two alternating pattern units,

the first being a rectangular unit such as jmnl, without any projections contained within the rectangle, and the second being a rectangular unit such as lnig with projection h at its center. One triangular unit of the pattern is typified by triangle abc wherein side $\overline{bc}$ is the shortest distance between projection centers and becomes D_1, while side $\overline{ca}$ is the perpendicular distance from side $\overline{bc}$ to the third projection center at "a" and becomes D_2. A second triangular unit is typified by triangle def in which sides $\overline{ef}$ and $\overline{de}$ are equal and are the shortest distance between projections centers of the triangle. Hence, side $\overline{ef}$ (or $\overline{de}$) becomes D_1 and the perpendicular distance from that side to the third projection center becomes D_2. A third triangular unit is typified by triangle ghi with sides $\overline{gh}$ and $\overline{hi}$ being equal and the shortest spacings between projection centers of the triangle. Hence, $\overline{gh}$ (or $\overline{hi}$) becomes D_1 and the perpendicular from a line containing such shortest side, and passing through the third projection center of the triangle becomes D_2. Triangle jkl may be constructed but does not meet the requirements of a triangular unit because side $\overline{kl}$ transverses shorter line segment $\overline{jm}$ interconnecting other projection centers. Accordingly, the D dimension for this projection pattern is determined by calculating the values for each of triangles abc, def and ghi, and selecting the largest of the three values.

EXAMPLE 4.

This invention may be compared with other heat exchanger configurations on the basis of adding various forms of metal to a basic automobile radiator unit consisting of 80 all-primary surface channels per foot heat exchanger cross section, each channel being 0.8 inch wide with 0.008 inch thick aluminum alloy as both primary and secondary surface metal. The coolant in the channels is 40% by weight ethylene glycol in water and the vehicle speed is 60 mph. The isostress-type wall projection portions are used in all heat exchangers of this example, having the following characteristics: projection spacings=0.6 inch horizontally and 0.5 inch vertically with effective D dimension of 0.39 inch, d=0.06 inch, and H=0.059 inch. Fig. 26 is a graph showing the forms of incremental metal as a percentage for additional heat transfer capacity to the basic unit, including additional primary surface as wider channels (curve A), smooth fins without surface distortions (curve B), single slat-slotted aperture louvered fins on each channel edge (curve D).

More specifically, the Fig. 26 graph shows the relationship between change in heat capacity per unit change in weight [Δ BTU/min. $\times$ft^2]/Δ lb. as the ordinate vs. added percentage of original heat exchanger weight as the abscissa. Curve A represents the change in heat capacity in an all-primary surface exchanger

as the channel width is increased from 0.8 inch to 1.5 inch, and the aspect ratio is increased from 12.4 (basic unit) to 21.8. Curve B illustrates the change in heat capacity when the same weights of metal are added as smooth fins rather than as additional all-primary surface wall. It is evident that there is only marginal difference between these two choices of incremental metal. Adding smooth fin shows a slight advantage up to about 40% additional weight and thereafter its contribution is actually smaller than obtained by equal weight additions of all-primary surface wall.

Curve C shows the change in heat capacity per unit weight of added metal when single, slat-slotted aperture louvered fins are added to the basic 0.8 inch wide channel. The previously defined angles for these fin surface distortions are as follows: $\alpha=65°$, $\beta=74°$, and $\gamma=56°$ and the slat dimension S is 0.083 inch. The ratio $(O_\sigma + O_\varepsilon)/I_T$ is increased from 1.5 to 2.8, corresponding respectively to 125% and 190% of the original heat exchanger weight. It is evident that indiscriminately adding large amounts of metal in any form would eventually reach a point of no advantage as the curves converge. However, it is also apparent that within the range of Fig. 26, i.e. up to about 90% by weight of incremental metal, the single, slat-slotted aperture louvered fins maintain at least a two-fold advantage over equal additions of all-primary metal as represented by curve A.

Curve D represents the addition of metal in the form of double, slat-slotted aperture louvered fins, and displays still better utility of added metal than realized with the single fins of curve C.

WHAT WE CLAIM IS:—

1. A cross flow heat exchanger comprising: an outer structural frame; a multiplicity of channels formed of aluminum each having an elongated cross section bound by side walls and edge walls each of between 0.003 and 0.015 inch thickness and an aspect ratio of length to width of an equivalent rectangle equal to at least 4, said channels being longitudinally aligned in parallel spaced relation each with a first fluid entrance opening at one end and a first fluid exit opening at the opposite end, and common inlet manifold means and common exit manifold means respectively for said first fluid entrance openings and said first fluid exit openings, and a multiplicity of wall projection portions formed from each side wall being distributed across the side wall surface and extending outwardly therefrom with load-bearing end segments shaped for mating with and abutting against load-bearing end segments of said projection portions of an adjacent channel side wall thereby spacing adjacent channels with the outermost end segments bearing against and transferring the channel load to said outer structural frame,

said wall projection portions having a dimensional size and a dimensional relationship therebetween defined by a D dimension of between about 0.2 and 1 inch, an H dimension of between about 0.02 and 0.14 inch, and a D/d ratio of between about 3 and 18 wherein H is the distance from each load-bearing end segment to the plane of the side wall surface in a direction perpendicular to said plane, D equals the effective spacing between the centers of adjacent wall projection portions of a side wall as determined by the formula:

$$D = 3\sqrt{\frac{D_1{}^3 + D_2{}^3}{2}}$$

wherein D_1=shortest distance between two adjacent wall projection portions in any triangular unit of the projection pattern on the side wall, D_2=perpendicular distance from a straight line extending through said two adjacent wall projection centers to the center of the third wall projection of the same triangular unit, triangular unit=a triangle having a wall projection center only at each of its apexes with each side of the triangle extending between wall projection centers without transversing a shorter line segment interconnecting other projection centers, and d equals the dimension of the ratio 4a/p wherein a equals the area of the load-bearing end segment of the wall-supporting projection and p equals the perimeter of said load-bearing end segment and said wall projection portions also having an elevational contour such that the ratio θ/R is between about 4 and 2500 degrees/inch wherein θ is the maximum angle of metal in the projection portion with respect to the base plane of said side wall and measured in a cross section passing through the projection portion center perpendicular to the base plane, and R is the minimum radius of curvature of said metal measured outside the projection portion; said channels and wall projection portions thereby, and outer structural frame being arranged and constructed for flowing a second fluid through said outer structural frame normal to and in the space between said channels in heat exchange with said first fluid; and at least one thin aluminum fin of between 0.003 and 0.015 inch thickness extending at least outwardly from an edge wall of each channel along the entire length thereof, said fins being provided in number and surface area relative to the channel surface area such that the ratio $(O_O + O_F)/I_T$ of channel outer surface area (O_O) plus fin surface area outside said channels (O_P) to total surface area inside said channels (I_T) is between 1.2 and 4.0, and with each fin having a multiplicity of surface distortions from the fin plane into the gap between adjacent fins of adjacent channels being closely spaced at intervals (S) between 0.01 and 0.2 inch measured normal to the channel

longitudinal axis, so as to comprise a total distortion area which is at least 40% of said fin surface area thereby disrupting the second fluid film across the fin width.

2. A cross flow heat exchanger according to claim 1 wherein the fin surface distortions comprise parallel slats and apertures arranged in a louvered configuration across the fin width.

3. A cross flow heat exchanger according to claim 1 wherein the fin surface distortions comprise a multiplicity of pleated strips across the fin width and separated by parallel slits, each pleated strip having crests and valleys with apertures formed by the strip edges between said crests and valleys, and with crests and valleys of adjacent pleated strips being nonaligned in the direction normal to said slits.

4. A cross flow heat exchanger according to claim 1 wherein the fin surface distortions comprise a series of corrugations having crests and valleys aligned parallel to the channel longitudinal axis and laterally spaced from each other.

5. A cross flow heat exchanger according to claim 1 wherein the fin surface distortions comprise dimples distributed over the fin surface and separated by undistorted metal, said dimples being aligned in longitudinal rows parallel to the channel longitudinal axis.

6. A cross flow heat exchanger according to any of claims 1 to 5 wherein at least one fin extends outwardly from each edge wall of each channel.

7. A cross flow heat exchanger according to any of claims 1 to 6 wherein two fins extend outwardly from each edge wall of each channel.

8. A cross flow heat exchanger according to any of claims 1 to 7 wherein the ratio $(O_O + O_F)/I_T$ is between 1.3 and 3.0.

9. A cross flow heat exchanger according to any of claims 1 to 8 wherein the fin surface distortions are spaced at intervals (S) between 0.02 and 0.10 inch.

10. A cross flow heat exchanger according to claim 2 wherein the channels are between 0.75 and 2.0 inch wide and the fins are between 0.2 and 0.5 inch wide.

11. A cross flow heat exchanger according to any of claims 1 to 10 wherein the aspect ratio of said channels is at least 8.

12. A cross flow heat exchanger according to any of claims 1 to 11 wherein the wall projection portions have an isostress elevational contour.

13. A cross flow heat exchanger according to any of claims 1 to 11 wherein the wall projection portions have a truncated cone elevational contour.

14. A cross flow heat exchanger according to any of claims 1 to 11 wherein the wall projection portions have an isostress contour and the fin surface distortions comprise parallel slats and apertures arranged in a louvered

configuration across the fin width.

15. A cross flow heat exchanger according to any of claims 1 to 14 wherein the wall projection portions have a D dimension of between about 0.3 and 0.85 inch, an H dimension of between about 0.025 and 0.1 inch, and a D/d ratio of between about 6 and 14.

16. A cross flow heat exchanger according to claim 1 or 15 wherein the wall projection portions have an isostress elevational contour such that the ratio θ/R is between about 4 and 100 degrees/inch.

17. A cross flow heat exchanger according to claim 2 wherein the slats are fabricated with an angle of approach θ' of between 0° and 60°, said angle of approach θ' of a slat being defined as the angle between a first line which is parallel to a plane containing the maximum dimensional width line and the longitudinal dimensional width line and the longitudinal dimensional length line of the channels and perpendicular to the channels' longitudinal length line, and a second line lying in the plane of the slat and in a plane normal to the surface of the slat and containing the first line as defined above.

18. A cross flow heat exchanger according to claim 18 wherein said angle of approach θ' is defined as the following:

$$\sin \theta' = (\cos \beta \times \sin \gamma - \cos \gamma \times \sin \beta \times \cos \alpha)$$

wherein

β is the angle formed between the plane of the fin and the plane of the slat member between adjacent slotted apertures;

γ is the angle formed between the plane of the fin and a plane containing the maximum width line and longitudinal length line of said channels; and

α is the angle formed between the longitudinal length line of the channels and the longitudinal length line of the slot formed between adjacent slats.

19. A cross flow heat exchanger according to claim 17 or 18 wherein said angle of approach θ' is between 0° and 45°.

20. A cross flow heat exchanger according to claim 18, wherein said angle of approach θ' is between 0 and 45°, the maximum dimensional width line of said channels is between 0.75 inch and 2.0 inches, and the fin width is less than 0.6 inch.

21. A cross flow heat exchanger according to claim 20 wherein the width of the slats of the louvered configuration are at least 0.02 inch.

22. A cross flow heat exchanger according to claim 20 wherein angle β is between 30° and 60°, angle α is between 45° and 135°, and angle γ is between 0° and 60°.

23. Cross flow heat exchangers constructed substantially as hereinbefore described with reference to Figs. 1 to 19C and 23 to 26 of the accompanying drawings.

W. P. THOMPSON & CO.,
12, Church Street,
Liverpool, L1 3AB.
Chartered Patent Agents.

F I G. 1

F I G. 2

F I G. 3

F I G. 4

F I G. 4A

F I G. 5D

F I G. 5A

F I G. 5B

F I G. 5C

F I G. 5

FIG. 5E

FIG. 9

FIG. 10

F I G. 7

F I G. 7A

F I G. 6

F I G. 8

F I G. 8A

F I G. 11

F I G. 11A

F I G. 13

F I G. 12

FIG. 14A   FIG. 14B   FIG. 14C

FIG. 14D   FIG. 14E   FIG. 14F
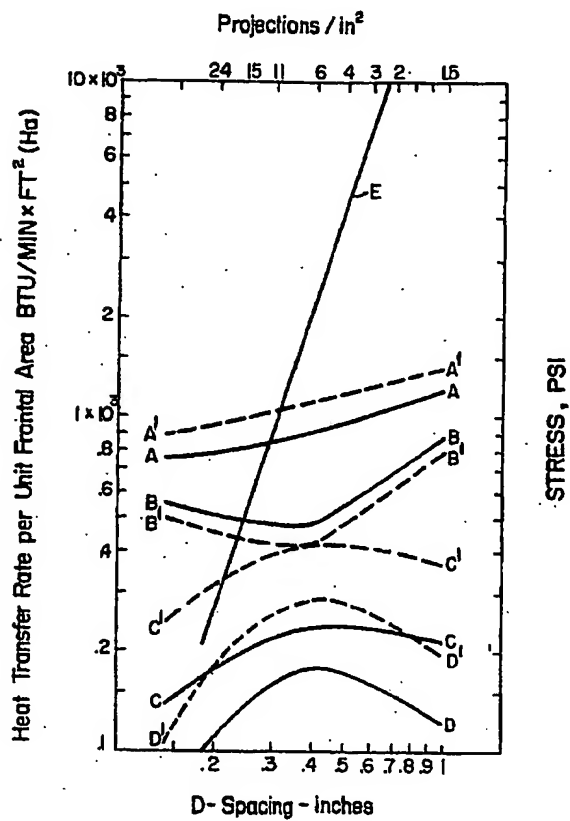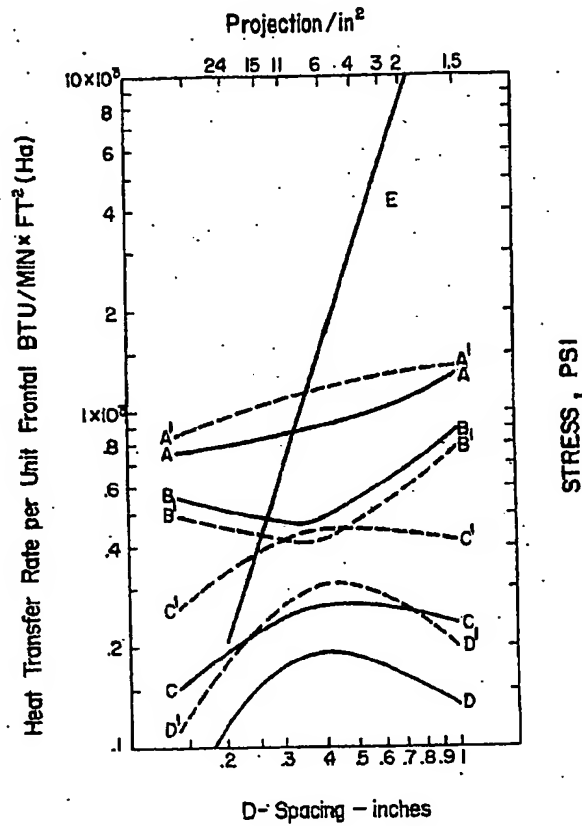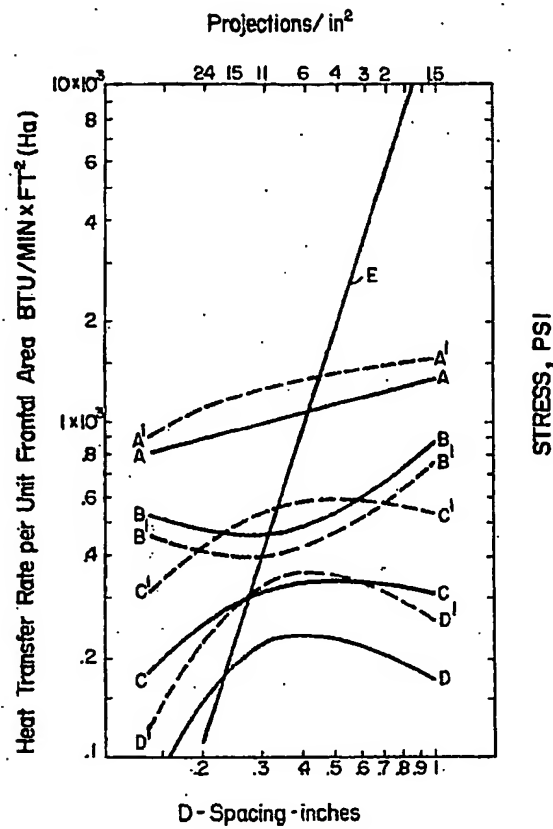
FIG. 14G   FIG. 14H

F I G. 15A

F I G. 15

F I G. 15B

1424689   COMPLETE SPECIFICATION
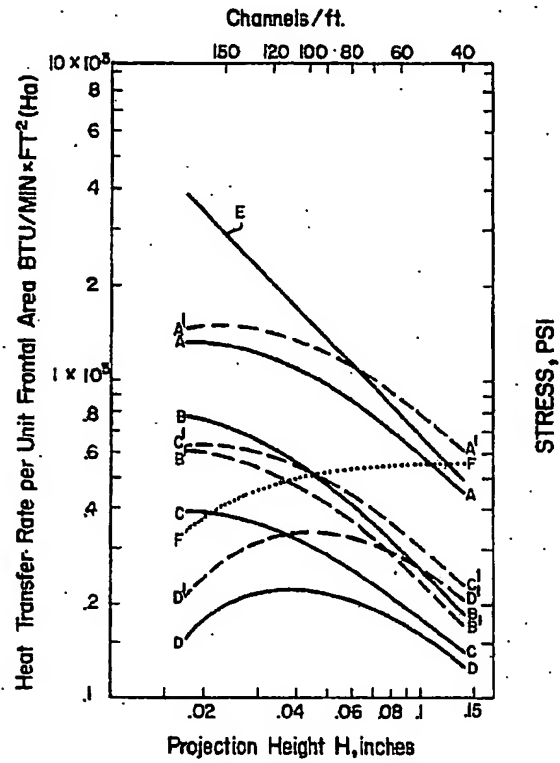22 SHEETS   *This drawing is a reproduction of
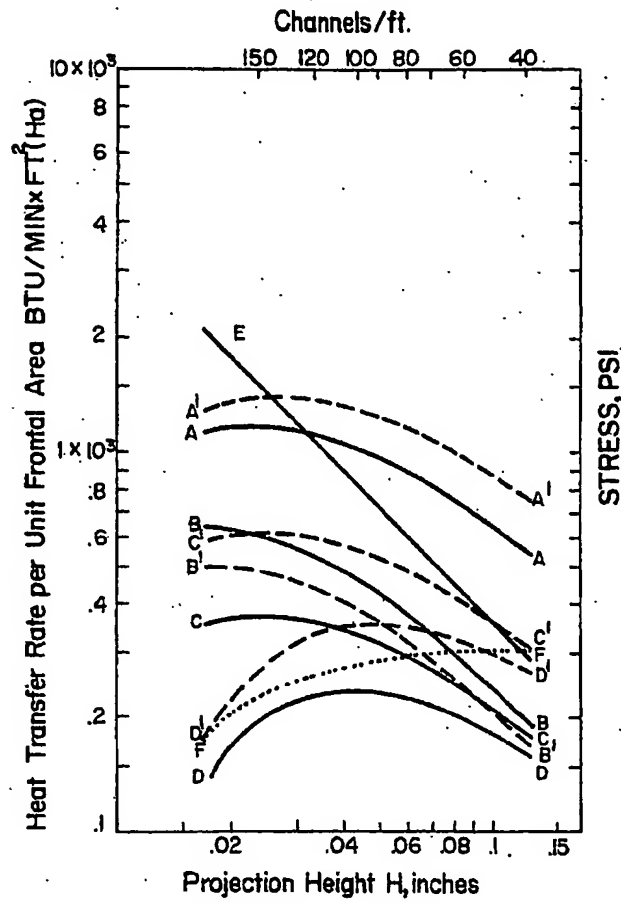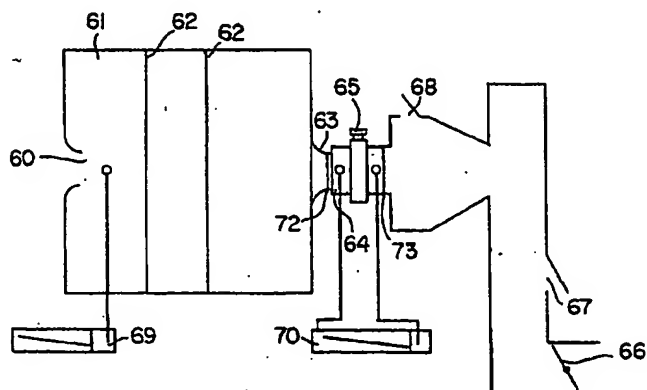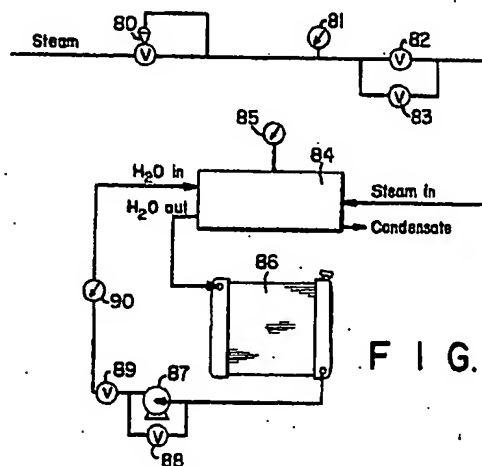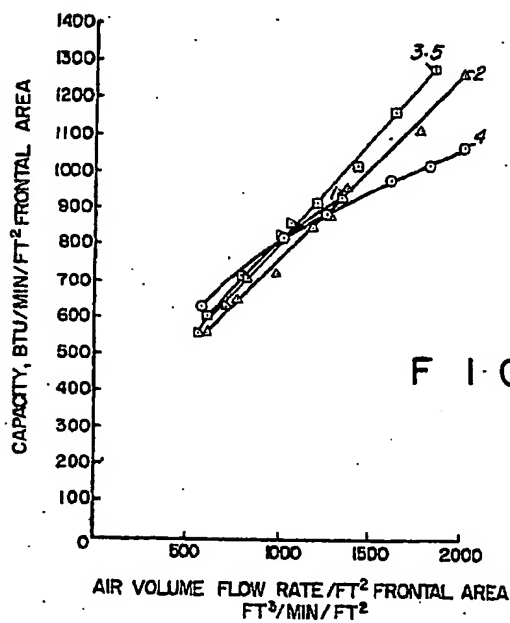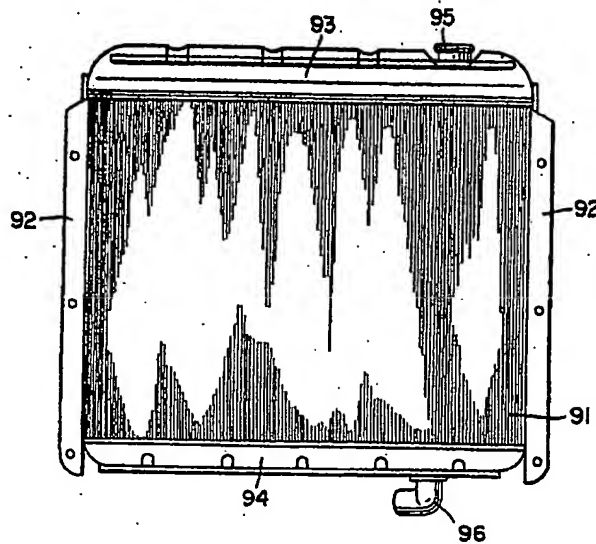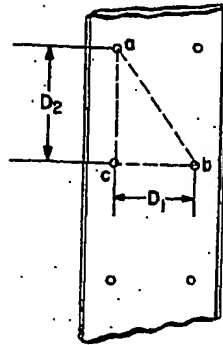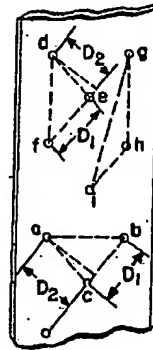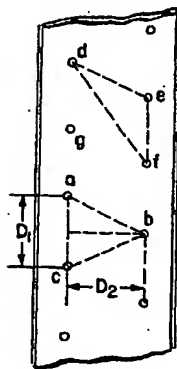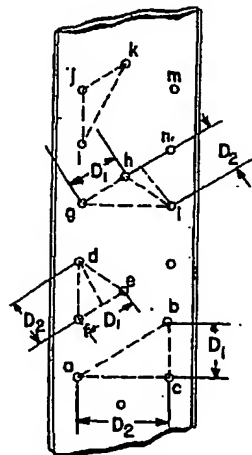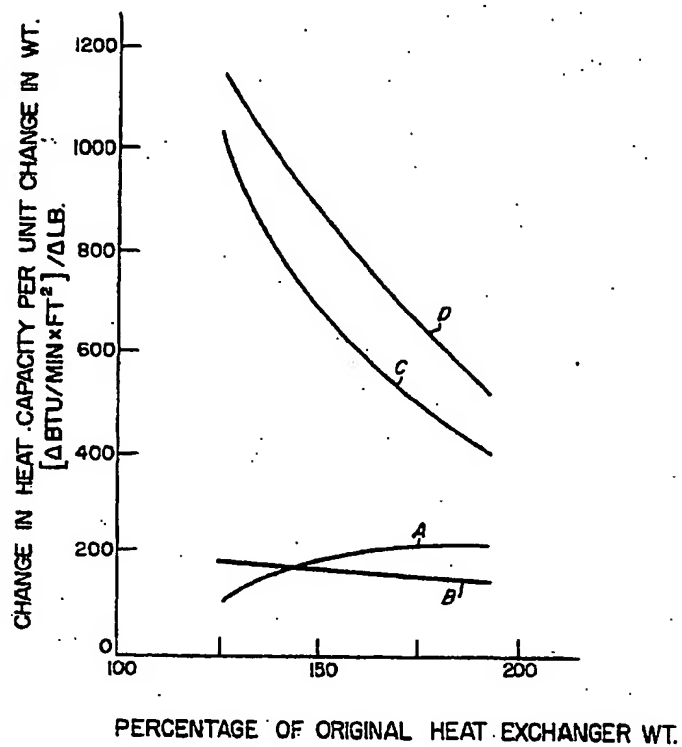the Original on a reduced scale*
Sheet 10

F I G. 16

FIG. 17

F I G. 18A

F. I G. 18B

F I G. 18C
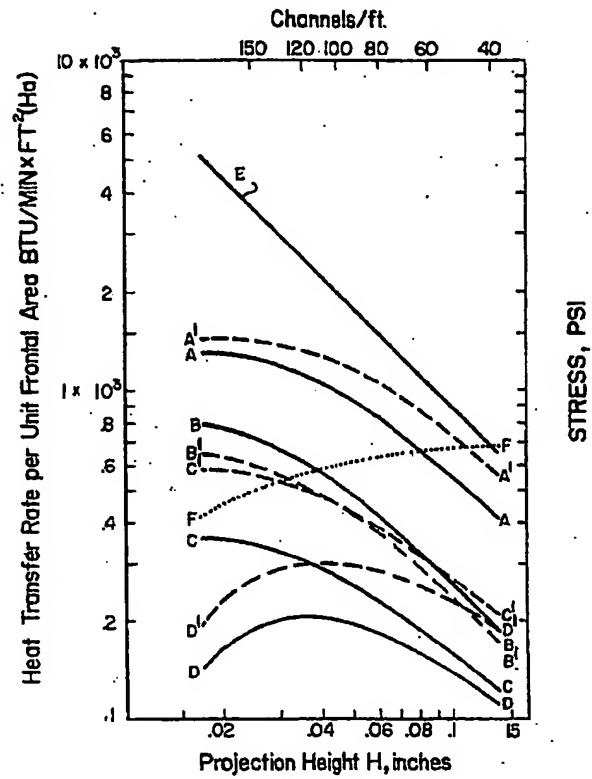
F I G.   19A

F I G. 19B

F I G.   19C

F I G. 20

F I G. 21

F I G. 22

F I G. 23

F I G.   24

F I G. 25A

F I G. 25B

F. I G. 25C

F I G. 25D

FIG. 26